UNIVERSITATEA DIN BUCUREȘTI
Facultatea de Fizică

Sebastian MICLUȚA-CÂMPEANU

LASER WAKEFIELD ACCELERATION
Studies using Particle in Cell Method

MASTER THESIS

Scientific Advisers
Prof. dr. Virgil BĂRAN
Conf. dr. Alexandru NICOLIN

Bucharest, 2019

Contents

Introduction

Add stuff here Tajima and Dawson 1979.

Chapter 1

Classical Electrodynamics

In order to study complex phenomena such as laser wakefield acceleration, we need to have a good understanding of the basic physical phenomena that govern the dynamics of charged particles in interaction with electromagnetic fields. In this thesis we will restrict ourselves to classical electrodynamics, ignoring QED effects that are important for very high laser intensities $I \gtrsim 5 \times 10^{22}\,\mathrm{W/cm^2}$. We will mainly follow the ideas presented in Jackson (1999) and Eisenberg and Greiner (1978, Chapter 2).

We thus begin with Maxwell's equations in free space

$$\boldsymbol{\nabla} \cdot \mathbf{E} = \frac{\rho}{\varepsilon_0} \tag{1.1a}$$

$$\boldsymbol{\nabla} \cdot \mathbf{B} = 0 \tag{1.1b}$$

$$\boldsymbol{\nabla} \times \mathbf{E} = -\frac{\partial \mathbf{B}}{\partial t} \tag{1.1c}$$

$$\boldsymbol{\nabla} \times \mathbf{B} = \mu_0 \mathbf{j} + \frac{1}{c^2}\frac{\partial \mathbf{E}}{\partial t}\,, \tag{1.1d}$$

which relate the electromagnetic field to sources. An additional equation must be satisfied in order to ensure charge conservation

$$\boldsymbol{\nabla} \cdot \mathbf{j}(\mathbf{r}, t) + \frac{\partial \rho(\mathbf{r}, t)}{\partial t} = 0\,. \tag{1.2}$$

As we can see above, equations (1.1b) and (1.1c) do not involve sources and thus they state the dynamical properties of the fields. Since equations (1.1a) and (1.1d) describe how the sources influence the fields, we need an additional equation to describe how the fields affect the sources

$$\mathbf{F} = \int \mathrm{d}\mathbf{r}'\, \rho(\mathbf{r}', t)\mathbf{E}(\mathbf{r}', t) + \frac{1}{c}\int \mathrm{d}\mathbf{r}'\, \mathbf{j}(\mathbf{r}', t) \times \mathbf{B}(\mathbf{r}', t)\,.$$

Maxwell's equations (1.1) relate six field quantities ($\mathbf{E}$ and $\mathbf{B}$) to four source quantities (ρ and $\mathbf{j}$). This implies that there are some restrictions on the six quantities. This suggests that we can find a less redundant way to express the fields, and indeed the four quantities given by the vector potential $\mathbf{A}$ and scalar potential ρ provide this representation. Equation (1.1b) implies the existence of a vector potential

$$\mathbf{B}(\mathbf{r}, t) = \boldsymbol{\nabla} \times \mathbf{A}(\mathbf{r}, t)\,. \tag{1.3}$$

Substituting (1.3) in (1.1c) we obtain

$$\boldsymbol{\nabla} \times \left(\mathbf{E} + \frac{\partial \mathbf{A}}{\partial t}\right) = 0 \tag{1.4}$$

and thus the quantity in the parenthesis can always be expressed as the gradient of a scalar field, namely the scalar potential

$$\boldsymbol{\nabla}\phi(\mathbf{r}, t) = -\mathbf{E}(\mathbf{r}, t) - \frac{\partial \mathbf{A}}{\partial t}.$$

With these considerations equation (1.1a) becomes

$$\boldsymbol{\nabla} \cdot \left(\boldsymbol{\nabla}\phi + \frac{\partial \mathbf{A}}{\partial t} \right) = -\frac{\rho}{\varepsilon_0}$$

or

$$\nabla^2 \phi + \frac{\partial}{\partial t} \boldsymbol{\nabla} \cdot \mathbf{A} = -\frac{\rho}{\varepsilon_0} \tag{1.5}$$

and equation (1.1d)

$$\boldsymbol{\nabla} \times (\boldsymbol{\nabla} \times \mathbf{A}) = \mu_0 \mathbf{j} - \frac{1}{c^2} \frac{\partial}{\partial t} \left(\boldsymbol{\nabla}\phi + \frac{\partial \mathbf{A}}{\partial t} \right). \tag{1.6}$$

Using the following vector identity

$$\boldsymbol{\nabla} \times (\boldsymbol{\nabla} \times \mathbf{A}) = \boldsymbol{\nabla}(\boldsymbol{\nabla} \cdot \mathbf{A}) - \nabla^2 \mathbf{A}, \tag{1.7}$$

equation (1.6) becomes

$$\boldsymbol{\nabla}(\boldsymbol{\nabla} \cdot \mathbf{A}) - \nabla^2 \mathbf{A} = \mu_0 \mathbf{j} - \frac{1}{c^2} \left(\boldsymbol{\nabla}\frac{\partial \phi}{\partial t} + \frac{\partial^2 \mathbf{A}}{\partial t^2} \right)$$

or

$$\nabla^2 \mathbf{A} - \frac{1}{c^2} \frac{\partial^2 \mathbf{A}}{\partial t^2} = -\mu_0 \mathbf{j} + \boldsymbol{\nabla}\left(\boldsymbol{\nabla} \cdot \mathbf{A} + \frac{1}{c^2} \frac{\partial \phi}{\partial t} \right). \tag{1.8}$$

Equations (1.5) and (1.8) were obtained by substituting the potentials obtained from the source-less equations, (1.1b) and (1.1c), into the ones with sources, (1.1a) and (1.1d). They are thus fully equivalent with Maxwell's equations (1.1) and, as we can observe, relate the four quantities given by the potentials to the four quantities for the sources. They also preserve the invariance under Lorentz transformations, with the scalar potential ϕ as the time-like component.

Equations (1.5) and (1.8) can be simplified by decoupling the potentials. This is possible due to the fact that potentials are not unique. To illustrate this point consider

$$\mathbf{A}'(\mathbf{r}, t) = \mathbf{A}(\mathbf{r}, t) + \boldsymbol{\nabla}\Lambda(\mathbf{r}, t).$$

This vector potential gives rise to a magnetic field

$$\mathbf{B}' = \boldsymbol{\nabla} \times \mathbf{A}' = \boldsymbol{\nabla} \times \mathbf{A} + \boldsymbol{\nabla} \times (\boldsymbol{\nabla}\Lambda) = \boldsymbol{\nabla} \times \mathbf{A} = \mathbf{B}$$

equal with the original one since $\boldsymbol{\nabla} \times (\boldsymbol{\nabla}\varphi) = 0$.

Similarly, for a scalar potential

$$\phi'(\mathbf{r}, t) = \phi(\mathbf{r}, t) - \frac{\partial \Lambda(\mathbf{r}, t)}{\partial t}$$

the corresponding electric field will be

$$\mathbf{E}' = -\boldsymbol{\nabla}\phi' - \frac{\partial \mathbf{A}'}{\partial t} = -\boldsymbol{\nabla}\phi + \boldsymbol{\nabla}\frac{\partial \Lambda}{\partial t} - \frac{\partial \mathbf{A}}{\partial t} - \frac{\partial}{\partial t}\boldsymbol{\nabla}\Lambda = -\boldsymbol{\nabla}\phi - \frac{\partial \mathbf{A}}{\partial t} = \mathbf{E},$$

since the spatial and temporal derivatives commute. These kinds of transformations are called gauge transformations.

1.1 Gauge transformations

The freedom of choosing the gauge leads to the following condition satisfied by the scalar and vector potentials

$$\boldsymbol{\nabla} \cdot \mathbf{A} + \frac{1}{c^2}\frac{\partial \phi}{\partial t} = 0 \,,$$

called the Lorenz condition.

Indeed, if we consider a set of potentials $\mathbf{A}$ and ϕ that don't satisfy the condition

$$\boldsymbol{\nabla} \cdot \mathbf{A} + \frac{1}{c^2}\frac{\partial \phi}{\partial t} \neq 0 = f(\mathbf{r},t) \,,$$

then we can always carry out a gauge transformation to a new set of potentials $\mathbf{A}'$ and ϕ' that satisfy the Lorenz condition, such that

$$\boldsymbol{\nabla} \cdot \mathbf{A} + \frac{1}{c^2}\frac{\partial \phi}{\partial t} = \boldsymbol{\nabla} \cdot (\mathbf{A}' - \boldsymbol{\nabla}\Lambda) + \frac{1}{c^2}\frac{\partial}{\partial t}\left(\phi' + \frac{\partial \Lambda}{\partial t}\right)$$

$$= \boldsymbol{\nabla} \cdot \mathbf{A}' - \nabla^2\Lambda + \frac{1}{c^2}\frac{\partial \phi'}{\partial t} + \frac{1}{c^2}\frac{\partial^2 \Lambda}{\partial t^2} = f(\mathbf{r},t)$$

or

$$\boldsymbol{\nabla} \cdot \mathbf{A} + \frac{1}{c^2}\frac{\partial \phi}{\partial t} = \Box\,\Lambda \equiv \frac{1}{c^2}\frac{\partial^2 \Lambda}{\partial t^2} - \nabla^2\Lambda = f(\mathbf{r},t) \,,$$

where the d'Alambertian operator is defined as

$$\Box \equiv \frac{1}{c^2}\frac{\partial^2}{\partial t^2} - \nabla^2$$

when choosing the Minkowski metric $(+,-,-,-)$ and

$$\boldsymbol{\nabla} \cdot \mathbf{A}' + \frac{1}{c^2}\frac{\partial \phi'}{\partial t} = 0 \,,$$

since they satisfy the Lorenz condition. The transformation we need is thus defined by the solution of $\Box\,\Lambda = f$.

Imposing the Lorenz condition on equations (1.5) and (1.4) decouples the potentials

$$\nabla^2\phi - \frac{\partial}{\partial t}\frac{1}{c^2}\frac{\partial \phi}{\partial t} = -\frac{\rho}{\varepsilon_0}$$

$$\nabla^2\mathbf{A} - \frac{1}{c^2}\frac{\partial^2 \mathbf{A}}{\partial t^2} = -\mu_0\mathbf{j}$$

yielding the simplified form of Maxwell's equations

$$\Box\,\phi = \frac{\rho}{\varepsilon_0}$$

$$\Box\,\mathbf{A} = \mu_0\mathbf{j} \,.$$

This form of Maxwell's equations preserves Lorentz invariance, since the Lorenz gauge condition can be expressed in a covariant way as the contraction of the four-vector $A \equiv (\frac{\phi}{c}, \mathbf{A})$ with the four-gradient $(\frac{1}{c}\frac{\partial}{\partial t}, -\boldsymbol{\nabla})$.

Since the Lorenz condition doesn't fix the gauge, but only restricts us to transformations with $\Box\,\Lambda = 0$, we can impose further conditions in order to fix the gauge, but in general those will not be covariant. One such condition is given by the Coulomb gauge

$$\boldsymbol{\nabla} \cdot \mathbf{A} = 0. \tag{1.9}$$

In this gauge equation (1.5) becomes a Poisson equation for the scalar potential

$$\nabla^2 \phi = -\frac{\rho}{\varepsilon_0} \tag{1.10}$$

with the solution given by the instantaneous Coulomb potential of the charge density in the domain $\rho(\mathbf{r}, t)$

$$\phi(\mathbf{r}, t) = \frac{1}{4\pi\varepsilon_0} \int \frac{\rho(\mathbf{r}', t)}{|\mathbf{r} - \mathbf{r}'|} \, \mathrm{d}\mathbf{r}' \,, \tag{1.11}$$

explaining the name of the condition (1.9).

An apparent violation of special relativity shows up in the above result which states that the scalar potential (at time t) is given by the instantaneous Coulomb interactions between charges (also at time t). The contradiction is only apparent and stems from the act that the Coulomb gauge is not Lorentz invariant.

In order to resolve the contradiction we first note that we can only observe the electric field

$$\mathbf{E}(\mathbf{r}, t) = -\boldsymbol{\nabla}\phi(\mathbf{r}, t) - \frac{\partial \mathbf{A}(\mathbf{r}, t)}{\partial t} \,.$$

Thus, the instantaneous propagation is removed by the time derivative of the vector potential.

In the Coulomb gauge, the vector potential is given by

$$\Box \mathbf{A} = \mu_0 \mathbf{j} - \frac{1}{c^2} \boldsymbol{\nabla} \frac{\partial \phi}{\partial t} \,. \tag{1.12}$$

Considering the continuity equation (1.2) and the form of the scalar potential in equation (1.11), the second term in equation (1.12) becomes

$$\boldsymbol{\nabla} \frac{\partial \phi}{\partial t} = \boldsymbol{\nabla} \frac{1}{4\pi\varepsilon_0} \int \frac{\frac{\partial \rho}{\partial t}}{|\mathbf{r} - \mathbf{r}'|} \, \mathrm{d}\mathbf{r}' = -\frac{1}{4\pi\varepsilon_0} \boldsymbol{\nabla} \int \frac{\boldsymbol{\nabla}' \cdot \mathbf{j}(\mathbf{r}', t)}{|\mathbf{r} - \mathbf{r}'|} \, \mathrm{d}\mathbf{r}' \,, \tag{1.13}$$

where $\boldsymbol{\nabla}'$ denotes the derivatives with respect to $\mathbf{r}'$. Using the Helmholtz decomposition we can write any sufficiently well behaved vector (the current density in this particular case) as the sum of a divergence-free (transversal) component and a curl-free (longitudinal) one:

$$\mathbf{j} = \mathbf{j}^t + \mathbf{j}^l \,,$$

where

$$\boldsymbol{\nabla} \cdot \mathbf{j}^t = 0$$
$$\boldsymbol{\nabla} \times \mathbf{j}^l = 0 \,.$$

Using the vector identity (1.7) and

$$\nabla^2 \frac{1}{|\mathbf{r} - \mathbf{r}'|} = -4\pi\delta(\mathbf{r} - \mathbf{r}')$$

we can write the current density as follows

$$\nabla^2 (\mathbf{j}^t + \mathbf{j}^l) = \boldsymbol{\nabla}(\boldsymbol{\nabla} \cdot \mathbf{j}^l) - \boldsymbol{\nabla} \times (\boldsymbol{\nabla} \times \mathbf{j}^t)$$
$$\int \frac{\nabla^2 \mathbf{j}}{|\mathbf{r} - \mathbf{r}'|} \, \mathrm{d}\mathbf{r}' = \int \frac{\boldsymbol{\nabla}(\boldsymbol{\nabla} \cdot \mathbf{j}^l)}{|\mathbf{r} - \mathbf{r}'|} \, \mathrm{d}\mathbf{r}' - \int \frac{\boldsymbol{\nabla} \times (\boldsymbol{\nabla} \times \mathbf{j}^t)}{|\mathbf{r} - \mathbf{r}'|} \, \mathrm{d}\mathbf{r}'$$
$$-4\pi\mathbf{j} = \underbrace{\boldsymbol{\nabla} \int \frac{\boldsymbol{\nabla} \cdot \mathbf{j}^l}{|\mathbf{r} - \mathbf{r}'|} \, \mathrm{d}\mathbf{r}'}_{-4\pi\mathbf{j}^l} - \underbrace{\boldsymbol{\nabla} \times \boldsymbol{\nabla} \times \int \frac{\mathbf{j}^t}{|\mathbf{r} - \mathbf{r}'|} \, \mathrm{d}\mathbf{r}'}_{4\pi\mathbf{j}^t}$$

5

and thus we obtain the two components as

$$\mathbf{j}^t = \frac{1}{4\pi}\boldsymbol{\nabla}\times\boldsymbol{\nabla}\times\int\frac{\mathbf{j}(\mathbf{r}',t)}{|\mathbf{r}-\mathbf{r}'|}\,\mathrm{d}\mathbf{r}'$$

$$\mathbf{j}^l = -\frac{1}{4\pi}\boldsymbol{\nabla}\int\frac{\boldsymbol{\nabla}'\cdot\mathbf{j}(\mathbf{r}',t)}{|\mathbf{r}-\mathbf{r}'|}\,\mathrm{d}\mathbf{r}'\,.$$

Comparing with equation (1.13) we see that

$$\frac{1}{c^2}\boldsymbol{\nabla}\frac{\partial\phi}{\partial t} = \frac{\varepsilon_0}{c^2}\mathbf{j}^l = \mu_0\mathbf{j}^l$$

and thus the source term in equation (1.12) can be expressed as function of the transverse current:

$$\Box\,\mathbf{A} = \mu_0(\mathbf{j}-\mathbf{j}^l) = \mu_0\mathbf{j}^t$$

and this also why the Coulomb gauge is also called the transverse gauge. This gauge is useful when no sources are present. In this case $\phi = 0$, $\mathbf{A}$ satisfies the homogeneous wave equation and the fields can be expressed only as function of the vector potential

$$\mathbf{E} = -\frac{\partial\mathbf{A}}{\partial t}$$

$$\mathbf{B} = \boldsymbol{\nabla}\times\mathbf{A}\,.$$

1.2   The Poynting theorem

In order to complete the description of the interaction between fields and sources, we will now focus on how the fields affect the particles. We begin by considering the force acting on a charge q

$$\mathbf{F} = q\mathbf{E} + q\mathbf{v}\times\mathbf{B}\,.$$

The corresponding infinitesimal variation of the force is given by

$$\delta\mathbf{F} = \rho\mathbf{E}\,\delta V + \mathbf{j}\times\mathbf{B}\,\delta V = (\rho\mathbf{E}+\mathbf{j}\times\mathbf{B})\,\delta V \equiv f\,\delta V\,,$$

where $f = \rho\mathbf{E}+\mathbf{j}\times\mathbf{B}$ is the Lorentz force density. We can now consider a uniform charge distribution characterized by ρ. For an infinitesimal volume δV of this charge distribution, the rate of change of the work, or the power given by the fields is given by

$$\mathbf{v}\cdot\mathbf{F} = \rho\mathbf{v}\mathbf{E} + \frac{\mathbf{j}}{q}\cdot(\mathbf{j}\times\mathbf{B}) = \rho\mathbf{v}\mathbf{E}\,.$$

As we can see above, the magnetic force doesn't contribute to the work done by the fields. Thus, the power transferred from the fields to the charges in a finite domain $\mathscr{D}$ is

$$\int_{\mathscr{D}}\mathbf{j}\cdot\mathbf{E}\,\mathrm{d}\mathbf{r}\,.$$

For the energy to be conserved, this power must be balanced by a corresponding rate of decrease of energy in the electromagnetic field. Using Ampère law (1.1d)

$$\int_{\mathscr{D}}\mathbf{j}\cdot\mathbf{E}\,\mathrm{d}\mathbf{r} = \int_{\mathscr{D}}\mathbf{E}\cdot\frac{1}{\mu_0}\left(\boldsymbol{\nabla}\times\mathbf{B}-\frac{1}{c^2}\frac{\partial\mathbf{E}}{\partial t}\right)\mathrm{d}\mathbf{r} = \frac{1}{\mu_0}\int_{\mathscr{D}}\left[\mathbf{E}\cdot(\boldsymbol{\nabla}\times\mathbf{B})-\frac{1}{c^2}\mathbf{E}\cdot\frac{\partial\mathbf{E}}{\partial t}\right]\mathrm{d}\mathbf{r}$$

Using the following vector identity

$$\nabla \cdot (\mathbf{E} \times \mathbf{B}) = \mathbf{B} \cdot (\nabla \times E) - \mathbf{E} \cdot (\nabla \times \mathbf{B})$$

we can express $\mathbf{E} \cdot (\nabla \times \mathbf{B})$ as

$$\mathbf{E} \cdot (\nabla \times \mathbf{B}) = \mathbf{B} \cdot (\nabla \times E) - \nabla \cdot (\mathbf{E} \times \mathbf{B}) = -\mathbf{B} \cdot \frac{\partial \mathbf{B}}{\partial t} - \nabla \cdot (\mathbf{E} \times \mathbf{B}),$$

where we used equation (1.1c) for the first term.

With these considerations, the power transferred by the fields is given by

$$\int_{\mathscr{D}} \mathbf{j} \cdot \mathbf{E}\, d\mathbf{r} = -\int_{\mathscr{D}} \left[\frac{1}{\mu_0} \nabla \cdot (\mathbf{E} \times \mathbf{B}) + \frac{1}{\mu_0} \mathbf{B} \cdot \frac{\partial \mathbf{B}}{\partial t} + \frac{1}{\mu_0 c^2} \mathbf{E} \cdot \frac{\partial \mathbf{E}}{\partial t} \right] d\mathbf{r}$$

Considering that

$$\mathbf{E} \cdot \frac{\partial \mathbf{E}}{\partial t} = \frac{1}{2} \frac{\partial}{\partial t} \mathbf{E}^2 \,,$$

we obtain

$$\int_{\mathscr{D}} \mathbf{j} \cdot \mathbf{E}\, d\mathbf{r} = -\int_{\mathscr{D}} \left[\frac{1}{2} \frac{\partial}{\partial t} \left(\varepsilon_0 \mathbf{E}^2 + \frac{1}{\mu_0} \mathbf{B}^2 \right) + \frac{1}{\mu_0} \nabla \cdot (\mathbf{E} \times \mathbf{B}) \right] d\mathbf{r} \,.$$

The total energy density of the electromagnetic field can be denoted with

$$w_{em} = \frac{1}{2} \left(\varepsilon_0 \mathbf{E}^2 + \frac{1}{\mu_0} \mathbf{B}^2 \right)$$

and thus we obtain

$$-\int_{\mathscr{D}} \mathbf{j} \cdot \mathbf{E}\, d\mathbf{r} = \int_{\mathscr{D}} \left[\frac{\partial w_{em}}{\partial t} + \frac{1}{\mu_0} \nabla \cdot (\mathbf{E} \times \mathbf{B}) \right] d\mathbf{r} \,.$$

Since the domain $\mathscr{D}$ is arbitrary, we can write the above as a differential continuity equation

$$\frac{\partial w_{em}}{\partial t} = -\nabla \cdot \mathbf{S} - \mathbf{j} \cdot \mathbf{E}, \tag{1.14}$$

where

$$\mathbf{S} = \frac{1}{\mu_0} \mathbf{E} \times \mathbf{B}$$

is the Poynting vector representing the energy flow.

If we consider the domain $\mathscr{D}$ such that no particles will leave it

$$W_{em} = \int_{\mathscr{D}} w_{em}\, d\mathbf{r}$$

is the energy of the electromagnetic field and W_{mech} is the energy of the particles

$$W_{mech} = \int_{\mathscr{D}} w_{mech}\, d\mathbf{r} = \int_{\mathscr{D}} \mathbf{j} \cdot \mathbf{E}\, d\mathbf{r} \,.$$

By using Gauss' theorem, the energy flux corresponding to the Poynting vector becomes

$$\int_{\mathscr{D}} \nabla \cdot \mathbf{S} = \oint_{\Sigma} \mathbf{n} \cdot \mathbf{S}\, da \,,$$

7

where Σ is the surface enclosing the domain $\mathscr{D}$.

With the above considerations Poynting's theorem gives the conservation of energy for the whole system

$$\frac{\mathrm{d}W}{\mathrm{d}t} = \frac{\mathrm{d}}{\mathrm{d}t}\left(W_{em} + W_{mech}\right) = -\oint_{\Sigma} \mathbf{n} \cdot \mathbf{S}\,\mathrm{d}a \, , \tag{1.15}$$

stating that the rate of change of the energy of the system composed of the charged particles and corresponding fields is given by minus the flux of the Poynting vector through the surface bounding the domain.

Equation (1.14) is the local form for the Poynting theorem.

If we consider the extension of the domain to infinity $\mathscr{D} \to \mathbb{R}^3$, $\Sigma \to \Sigma_{\infty}$, then there is no energy flow through the boundary since electromagnetic waves propagate at a constant finite speed c. Then

$$\frac{\mathrm{d}W}{\mathrm{d}t} = \frac{\mathrm{d}}{\mathrm{d}t}\left(W_{em} + W_{mech}\right) = 0$$

and the entire energy of the electromagnetic field can be converted into the mechanical energy of the particles interacting with the field.

If we consider $\mathscr{D}$ such that it doesn't enclose any sources, than

$$\frac{\mathrm{d}}{\mathrm{d}t}W_{em} = -\oint_{\Sigma} \mathbf{n} \cdot \mathbf{S}\,\mathrm{d}a \, ,$$

which shows that the energy of the electromagnetic field in the domain $\mathscr{D}$ can change through the variation of the flux of the Poynting vector on the boundary of the domain, Σ. Thus we can indeed say that the flux of the Poynting vector is the energy flux.

1.3   Electromagnetic waves

In the absence of sources, Maxwell's equations become

$$\boldsymbol{\nabla} \cdot \mathbf{B} = 0 \qquad \boldsymbol{\nabla} \times \mathbf{E} + \frac{\partial \mathbf{B}}{\partial t} = 0$$
$$\boldsymbol{\nabla} \cdot \mathbf{D} = 0 \qquad \boldsymbol{\nabla} \times \mathbf{H} - \frac{\partial \mathbf{D}}{\partial t} = 0 \, ,$$

where $\mathbf{D} = \varepsilon \mathbf{E}$, $\mathbf{B} = \mu \mathbf{H}$ and $\mathbf{D}$ is the displacement field and $\mathbf{H}$ is the magnetizing field. In our case, $\varepsilon = \varepsilon_0$ and $\mu = \mu_0$.

If we assume that the time dependence for the solutions is given by $\mathrm{e}^{-\mathrm{i}\omega t}$, then the above equations become

$$\boldsymbol{\nabla} \cdot \mathbf{B} = 0 \qquad \boldsymbol{\nabla} \times \mathbf{E}\,\mathrm{e}^{-\mathrm{i}\omega t} -\mathrm{i}\omega \mathbf{B}\,\mathrm{e}^{-\mathrm{i}\omega t} = 0$$
$$\boldsymbol{\nabla} \cdot \mathbf{D} = 0 \qquad \boldsymbol{\nabla} \times \mathbf{H}\,\mathrm{e}^{-\mathrm{i}\omega t} +\mathrm{i}\omega \mathbf{D} = 0 \, .$$

More complex time dependencies can be treated with a Fourier decomposition since if we have a solution, any linear combinations with that solution are also solutions.

If we consider only the curl equations

$$\boldsymbol{\nabla} \times \mathbf{E} - \mathrm{i}\omega \mathbf{B} = 0$$
$$\boldsymbol{\nabla} \times \mathbf{B} + \mathrm{i}\omega\mu\epsilon \mathbf{E} = 0$$

and take the curl

$$\boldsymbol{\nabla} \times \boldsymbol{\nabla} \times \mathbf{E} - \mathrm{i}\omega \boldsymbol{\nabla} \times \mathbf{B} = \boldsymbol{\nabla} \underbrace{(\boldsymbol{\nabla} \cdot \mathbf{E})}_{0} - \nabla^2 \mathbf{E} + (\mathrm{i}\omega)^2 \mu\varepsilon \mathbf{E} = 0$$

we obtain the Helmholtz wave equations

$$\left(\nabla^2 + \omega^2 \mu\varepsilon\right) \mathbf{E} = 0$$
$$\left(\nabla^2 + \omega^2 \mu\varepsilon\right) \mathbf{B} = 0$$

or in a more compact notation

$$\left(\nabla^2 + \omega^2 \mu\varepsilon\right) \begin{pmatrix} \mathbf{E} \\ \mathbf{B} \end{pmatrix} = 0 \,.$$

Taking the plane wave

$$\mathrm{e}^{\mathrm{i}kx - \mathrm{i}\omega t}$$

as a solution for the Helmholtz wave equation (1.3), we can study what properties arise for wave number k and the frequency ω. Thus we can see that

$$-k^2 + \omega^2 \mu\varepsilon = 0$$

or

$$k = \omega\sqrt{\mu\varepsilon} \,.$$

The phase velocity of a wave v_ϕ is defined as

$$v_\phi = \frac{\omega}{k} \,.$$

In this case, the phase velocity of a plane wave satisfying the Helmholtz equation is

$$v_\phi = \frac{1}{\sqrt{\mu\varepsilon}} = \frac{c}{n} \,,$$

where n is the refraction index of the media in which the wave propagates and is given by

$$n = \sqrt{\frac{\mu}{\mu_0} \frac{\varepsilon}{\varepsilon_0}} \,.$$

A general solution for the wave equation can be constructed by using the superposition principle

$$u(x,t) = a\,\mathrm{e}^{\mathrm{i}kx - \mathrm{i}\omega t} + b\,\mathrm{e}^{-\mathrm{i}kx - \mathrm{i}\omega t} \,.$$

This general solution can be seen as a superposition of incoming and outgoing plane waves.

Let us now consider an electromagnetic plane wave, that is a plane wave that satisfies both the Helmholtz wave equation (1.3) and Maxwell's equations (1.1)

$$\mathbf{E}(\mathbf{x}, t) = \boldsymbol{\mathcal{E}}\,\mathrm{e}^{\mathrm{i}k\mathbf{n}\cdot\mathbf{x} - \mathrm{i}\omega t}$$
$$\mathbf{B}(\mathbf{x}, t) = \boldsymbol{\mathcal{B}}\,\mathrm{e}^{\mathrm{i}k\mathbf{n}\cdot\mathbf{x} - \mathrm{i}\omega t} \,.$$

First, let us consider the Laplacian in the Helmholtz equation

$$\frac{\partial^2}{\partial x_i^2} \mathcal{E}_i\,\mathrm{e}^{\mathrm{i}kn_j x_j - \mathrm{i}\omega t} = \frac{\partial}{\partial x_i} \mathrm{i}kn_j \delta_{ij} \mathcal{E}_i\,\mathrm{e}^{\mathrm{i}kn_j x_j - \mathrm{i}\omega t} = -k^2 n_i n_i \mathcal{E}_i\,\mathrm{e}^{\mathrm{i}kn_j x_j - \mathrm{i}\omega t} \,.$$

With this consideration, Helmholtz equation yields

$$-k^2 n_i n_i \mathcal{E}_i \, \mathrm{e}^{\mathrm{i}kn_j x_j - \mathrm{i}\omega t} + \mu\varepsilon\omega^2 \mathcal{E}_i \, \mathrm{e}^{\mathrm{i}kn_j x_j - \mathrm{i}\omega t} = 0$$

or

$$k^2 \mathbf{n} \cdot \mathbf{n} = \mu\varepsilon\omega^2 \,.$$

Considering that $k = \sqrt{\mu\varepsilon}\,\omega$, we obtain that the norm of $\mathbf{n}$ must be 1

$$\mathbf{n} \cdot \mathbf{n} = 1 \,.$$

Now we continue with Maxwell's equations. We begin with the divergence equations

$$\boldsymbol{\nabla} \cdot \mathbf{B} = 0 \implies \partial_i \mathcal{B}_i \, \mathrm{e}^{\mathrm{i}kn_j x_j - \mathrm{i}\omega t} = 0 \,,$$

where we have used the notation

$$\partial_i \equiv \frac{\partial}{\partial x_i} \,.$$

Thus $\mathrm{i}kn_i \mathcal{B}_i = 0$ and the magnetic field $\mathbf{B}$ and $\mathbf{n}$ are perpendicular since

$$\mathbf{n} \cdot \boldsymbol{\mathcal{B}} = 0 \,.$$

Similarly, for the electric field

$$\boldsymbol{\nabla} \cdot \mathbf{D} = 0 \implies \partial_i \varepsilon \mathcal{E}_i \, \mathrm{e}^{\mathrm{i}kn_j x_j - \mathrm{i}\omega t} = 0$$

and

$$\mathrm{i}kn_i \mathcal{E}_i = 0 \implies \mathbf{n} \cdot \boldsymbol{\mathcal{E}} = 0 \,.$$

Thus, since the electric and magnetic fields are perpendicular to the propagation direction given by the $\mathbf{n}$ versor, the electromagnetic plane wave is a transverse wave.

If we now consider the curl equation

$$\boldsymbol{\nabla} \times \mathbf{E} = -\frac{\partial \mathbf{B}}{\partial t} \,,$$

we obtain

$$\varepsilon_{ijk} \partial_j E_k = -(-\mathrm{i}\omega)\mathcal{B}_i \, \mathrm{e}^{\mathrm{i}kn_i x_i - \mathrm{i}\omega t}$$
$$\varepsilon_{ijk} \partial_j \mathcal{E}_k \, \mathrm{e}^{\mathrm{i}kn_i x_i - \mathrm{i}\omega t} = \mathrm{i}\omega \mathcal{B}_i \, \mathrm{e}^{\mathrm{i}kn_i x_i - \mathrm{i}\omega t}$$
$$\varepsilon_{ijk} \mathcal{E}_k \mathrm{i}kn_j = \mathrm{i}\omega \mathcal{B}_i \,.$$

Thus $\mathbf{n} \times \boldsymbol{\mathcal{E}}\sqrt{\mu\varepsilon} = \boldsymbol{\mathcal{B}}$ or

$$\mathbf{n} \times \boldsymbol{\mathcal{E}}\frac{n}{c} = \boldsymbol{\mathcal{B}} \,.$$

In vacuum ($n = 1$), we observe that the electric and magnetic field differ in magnitude by a factor of c

$$|\boldsymbol{\mathcal{E}}| = |c\boldsymbol{\mathcal{B}}| \,. \tag{1.18}$$

If we consider a coordinate system spanned by the versors $(\boldsymbol{\epsilon}_1, \boldsymbol{\epsilon}_2, \mathbf{n})$, then the electric and magnetic field magnitudes can be written as

$$\boldsymbol{\mathcal{E}} = \boldsymbol{\epsilon}_1 E_0 \qquad \boldsymbol{\mathcal{B}} = \boldsymbol{\epsilon}_2 \sqrt{\mu\varepsilon} E_0 \,.$$

A plane wave with its electric field always in a direction $\boldsymbol{\epsilon}_1$ is called *linearly polarized* with the polarization vector $\boldsymbol{\epsilon}_1$.

According to the Poynting theorem, the plane wave transports energy. The Poynting vector in this case is given by

$$\mathbf{S} = \mathbf{E} \times \mathbf{H} = \mathbf{e}_i \varepsilon_{ijk} \boldsymbol{\epsilon}_{1j} E_0 \boldsymbol{\epsilon}_{2k} \frac{1}{\mu}\sqrt{\mu\varepsilon} = \sqrt{\frac{\varepsilon}{\mu}} E_0^2 \mathbf{n}$$

1.4 Electron in a Plane Wave

In this section we will consider the classical dynamics of an electron in a linearly polarized laser pulse following the discussion in Karsch (2018). We will assume an electron in vacuum and we will consider that the fields vary only along the Ox direction and explore the motion in the non-relativistic and relativistic cases. Thus the vector potential will be

$$\mathbf{A}(x,t) = \mathbf{e}_y A_0 \sin(kx - \omega t) \tag{1.19}$$

and the electric and magnetic fields will be given by

$$\mathbf{E}(x,t) = -\frac{\partial \mathbf{A}}{\partial t} - \underbrace{\boldsymbol{\nabla}\phi}_{0} = \mathbf{e}_y E_0 \cos(kx - \omega t)$$

$$\mathbf{B}(x,t) = \frac{\partial A_y}{\partial x}\mathbf{e}_z = \mathbf{e}_z B_0 \cos(kx - \omega t)\,,$$

where $E_0 = \omega A_0$ and $B_0 = kA_0$.

1.4.1 Non-relativistic treatment

In the non-relativistic case, the Lorentz force that gives the equation of motion for the electron is described by

$$\frac{\mathrm{d}\mathbf{p}}{\mathrm{d}t} = -e\left[\mathbf{E}(x,t) + \mathbf{v} \times \mathbf{B}(x,t)\right]\,. \tag{1.20}$$

As we noted in equation (1.18), the magnetic field amplitude is c times less than the one of the electric field and thus the second term in equation (1.20) can be ignored, since its magnitude is proportional to v/c, and in the non-relativistic case this ratio goes to 0. The equation of motion can be now solved by integration yielding

$$\mathbf{p} = -e\int \mathbf{E}(x,t)\mathrm{d}t\,.$$

Considering the electron is at rest at $t = 0$, its velocity will be given by

$$\mathbf{v} = \mathbf{e}_y \frac{eE_0}{\omega m_e} \sin(kx - \omega t)\,.$$

We can observe that the maximum velocity for the electron in this case is given by

$$v_{max} = \frac{eE_0}{\omega m_e}\,.$$

This gives us an estimate for how far can the non-relativistic approximation can go since at $v_{max} = c$ it will no longer be valid (actually it will be erroneous well before reaching the breaking point). Thus, at the breaking point, the relativistic factor $\beta = v/c$ will be unity and

$$\beta_{max} \equiv \frac{v_{max}}{c} = \frac{eE_0}{\omega m_e c} = \frac{eA_0}{m_e c} \equiv a_0\,,$$

where a_0 is called the normalized vector potential and can be used to measure how "relativistic" is the electron motion in the corresponding electric field. We can thus use it to estimate the

laser intensities up to which the non-relativistic description is valid. Considering $a_0 = 1$ we express the electric field magnitude as

$$E_0 = a_0 \frac{\omega m_e c}{e} = \frac{a_0}{\lambda} 2\pi \frac{m_e c^2}{e}.$$

Since laser wavelengths are usually expressed in µm, it can be useful to write the above as

$$E_0 = \frac{a_0}{\lambda} 3.21 \times 10^{12} \, \mathrm{V \, m^{-1} \, \mu m}.$$

Similarly, the magnetic field will be given by

$$B_0 = \frac{E_0}{c} = \frac{a_0}{\lambda} 1.07 \times 10^{18} \, \mathrm{T \, \mu m}.$$

Thus the limiting laser intensity for the non-relativistic description will be around

$$I = \frac{\varepsilon_0 c}{2} E_0^2 = \frac{a_0^2}{\lambda^2} 1.37 \times 10^{18} \, \mathrm{W \, cm^{-2} \, \mu m^2},$$

where we have used **??**. Thus for laser intensities above $10^{18} \, \mathrm{W \, cm^{-2}}$, the motion must be treated relativistically.

1.4.2 Relativistic treatment

We will now continue with the relativistic case, where the equation of motion is changed by the fact that the momentum of the electron is given by

$$\mathbf{p} = \gamma m_e \mathbf{v},$$

where

$$\gamma = \frac{1}{\sqrt{1 - \frac{v^2}{c^2}}} = \frac{1}{1 - \beta^2}.$$

Thus the equation of motion will be

$$\frac{\mathrm{d}\mathbf{p}}{\mathrm{d}t} = \frac{\mathrm{d}}{\mathrm{d}t}(\gamma m_e \mathbf{v}) = -e(\mathbf{E} + \mathbf{v} \times \mathbf{B}). \tag{1.21}$$

The γ factor can also be written as a function of the momenta

$$\gamma = \frac{1}{\sqrt{1 - \frac{v^2}{c^2}}} \implies \gamma^2 \left(1 - \frac{v^2}{c^2}\right) = 1$$

$$\text{or } \gamma^2 = 1 + \gamma^2 \frac{v^2}{c^2}$$

$$\gamma = \sqrt{1 + \gamma^2 \frac{v^2}{c^2}} \implies \gamma = \sqrt{1 + \left(\frac{\mathbf{p}}{m_e c}\right)^2}.$$

The time derivative of the γ factor is thus given by

$$\frac{\mathrm{d}\gamma}{\mathrm{d}t} = \frac{\mathrm{d}}{\mathrm{d}t}\sqrt{1 + \left(\frac{\mathbf{p}}{m_e c}\right)^2} = \frac{1}{\gamma}\frac{\mathrm{d}}{\mathrm{d}t}\left(\frac{\mathbf{p}}{m_e c}\right)^2 = \frac{1}{2\gamma}\frac{1}{(m_e c)^2}\frac{\mathrm{d}\mathbf{p}^2}{\mathrm{d}t},$$

where the time derivative of the square of the momenta can also be expressed as

$$\frac{1}{2}\frac{d\mathbf{p}^2}{dt} = \mathbf{p}\cdot\frac{d\mathbf{p}}{dt} = -e\mathbf{p}\cdot\mathbf{E} - e\underbrace{\mathbf{p}\cdot(\mathbf{v}\times\mathbf{B})}_{0} = -e\mathbf{p}\cdot\mathbf{E}\,.$$

With this consideration, the time derivative for γ yields

$$\frac{d\gamma}{dt} = \frac{1}{\gamma}\frac{1}{(m_e c)^2}(-e\mathbf{p}\cdot\mathbf{E})\,. \tag{1.22}$$

The relativistic kinetic energy is given by $E_{kin} = (\gamma - 1)m_e c^2$ and thus its time derivative can be easily computed with the aid of equation (1.22)

$$\frac{dE_{kin}}{dt} = m_e c^2\frac{d\gamma}{dt} = m_e c^2\frac{1}{\gamma}\frac{1}{(m_e c)^2}(-e\mathbf{p}\cdot\mathbf{E}) = -\frac{1}{\gamma m_e}e\mathbf{p}\cdot\mathbf{E}$$

or

$$\frac{dE_{kin}}{dt} = -e\mathbf{v}\cdot\mathbf{E}\,. \tag{1.23}$$

We will now the equation of motion for the electron and we will begin with the particular case of the O_y component of the motion. Let us now consider the following

$$\mathbf{E} = -\frac{\partial\mathbf{A}}{\partial t} = -\frac{d\mathbf{A}}{dt} + \underbrace{\frac{\partial\mathbf{A}}{\partial\mathbf{x}}\frac{\partial\mathbf{x}}{\partial t}}_{(\mathbf{v}\cdot\boldsymbol{\nabla})\mathbf{A}}$$

$$\mathbf{v}\times\mathbf{B} = \mathbf{v}\times(\boldsymbol{\nabla}\times\mathbf{A}) = \boldsymbol{\nabla}(\mathbf{v}\cdot\mathbf{A}) - (\mathbf{v}\cdot\boldsymbol{\nabla})\mathbf{A}\,,$$

then equation (1.21) becomes

$$\frac{d\mathbf{p}}{dt} = -e\left[-\frac{d\mathbf{A}}{dt} + (\mathbf{v}\cdot\boldsymbol{\nabla})\mathbf{A} + \boldsymbol{\nabla}(\mathbf{v}\cdot\mathbf{A}) - (\mathbf{v}\cdot\boldsymbol{\nabla})\mathbf{A}\right] = e\frac{d\mathbf{A}}{dt} - e\boldsymbol{\nabla}(\mathbf{v}\cdot\mathbf{A})\,.$$

With the considerations in equation (1.19), $\mathbf{A} = \mathbf{e}_y A_0\sin\phi$, where $\phi = kx - \omega t$, the $\mathbf{v}\cdot\mathbf{A}$ term becomes

$$\mathbf{v}\cdot\mathbf{A} = v_y A_0\sin\phi\,.$$

Since we are dealing with a plane wave, the velocity and the vector potential are independent and thus

$$\frac{\partial}{\partial y}(v_y A_0) = \frac{\partial}{\partial z}(v_y A_0) = 0\,.$$

The equation of motion for the electron for the O_y direction is then given by

$$\frac{dp_y}{dt} = e\frac{dA}{dt}$$

with the solution

$$p_y - eA = \mathcal{C}_1\,. \tag{1.24}$$

We can observe that $\mathcal{C}_1$ is a constant of the motion. In the case where the electron is initially at rest, $p_y = eA$.

Having emphasized the existence of the constants of the motion $\mathcal{C}_1$, we now move on to the complete equation of motion, which reads

$$\frac{d\tilde{\mathbf{p}}}{dt} = \frac{d}{dt}\begin{pmatrix}\tilde{p}_x\\\tilde{p}_y\\\tilde{p}_z\end{pmatrix} = -\frac{e}{m_e c}\left[\begin{pmatrix}0\\E_0\\0\end{pmatrix} + \begin{pmatrix}v_x\\v_y\\v_z\end{pmatrix}\times\begin{pmatrix}0\\0\\B_0\end{pmatrix}\right]\cos\phi\,,$$

13

where we have used the notation $\tilde{p} \equiv \frac{p}{m_e c}$. The above equation can be further expanded into

$$
\begin{aligned}
\frac{\mathrm{d}\tilde{\mathbf{p}}}{\mathrm{d}t} &= -\frac{e}{m_e c}\left[\begin{pmatrix} 0 \\ E_0 \\ 0 \end{pmatrix} + \begin{pmatrix} v_y B_0 \\ -v_x B_0 \\ 0 \end{pmatrix}\right]\cos\phi \\
&= -\frac{eE_0}{m_e c}\left[\begin{pmatrix} 0 \\ 1 \\ 0 \end{pmatrix} + \begin{pmatrix} v_y/c \\ -v_x/c \\ 0 \end{pmatrix}\right]\cos\phi \\
&= -a_0\omega \begin{pmatrix} v_y/c \\ 1 - v_x/c \\ 0 \end{pmatrix}\cos\phi .
\end{aligned}
\tag{1.25}
$$

Another constant of the motion can be found by considering the energy equation (1.23). The time derivative of the γ factor yields

$$
\begin{aligned}
\frac{\mathrm{d}\gamma}{\mathrm{d}t} &= -\frac{e}{m_e c^2}\mathbf{v}\cdot\begin{pmatrix} 0 \\ E_0 \\ 0 \end{pmatrix}\cos\phi \\
&= -\frac{eE_0}{m_e c}\frac{v_y}{c}\cos\phi = -a_0\omega\frac{v_y}{c}\cos\phi
\end{aligned}
$$

and we can thus express it using the normalised vector potential a_0.

Taking a look at the O_x direction component of the equation of motion and the O_y direction component of the energy equation shows some similarities

$$
\frac{\mathrm{d}\tilde{p}_x}{\mathrm{d}t} = -a_0\omega\frac{v_y}{c}\cos\phi = \frac{\mathrm{d}\gamma}{\mathrm{d}t} .
$$

Thus

$$
\frac{\mathrm{d}}{\mathrm{d}t}(\tilde{p}_x - \gamma) = 0 \implies \gamma - \tilde{p}_x = \mathcal{C}_2
\tag{1.26}
$$

we find a second constant of the motion $\mathcal{C}_2$, whose values depend on the initial conditions. Considering the electron at rest at $t = 0, x = 0$, then $\mathbf{p} = 0$, $\gamma = 1$ and $\mathcal{C}_2 = 1$. With this result we can see that at other times t that $\gamma = 1 + \tilde{p}_x$. We observe that the square of the γ factor can be written both as

$$
\gamma^2 = \left(\sqrt{1 + \left(1 + \frac{p}{m_e c}\right)^2}\right)^2 = 1 + \left(1 + \frac{p}{m_e c}\right)^2 = 1 + \tilde{\mathbf{p}}^2
$$

and as

$$
\gamma^2 = (1 + \tilde{p}_x)^2 .
$$

Moreover, since from equation (1.25) $p_z = 0$ for all times

$$
1 + \tilde{p}_x^2 + \tilde{p}_y^2 + \underbrace{\tilde{p}_z^2}_{0} = 1 + 2\tilde{p}_x + \tilde{p}_x^2
$$

$$
\tilde{p}_y^2 = 2\tilde{p}_x
$$

and thus we obtain a relation between forward momenta and transverse momenta

$$
\tilde{p}_x = \frac{1}{2}\tilde{p}_y^2 .
\tag{1.27}
$$

Taking into account equations (1.24), (1.26) and (1.27), the kinetic energy can be written as

$$E_{kin} = (\gamma - 1)m_e c^2 = (1 + \tilde{p}_x - 1)m_e c^2 = \frac{1}{2}\tilde{p}_y^2 m_e c^2 = \frac{1}{2}\underbrace{\left(\frac{eA}{m_e c}\right)^2}_{a^2} m_e c^2\,,$$

where the a notation was used similarly to the normalized vector potential a_0. With this notation, the kinetic energy relation has a formal similarity with the classical one

$$E_{kin} = m_e c^2 \frac{a^2}{2}$$

considering that $\tilde{p}_y = a$.

Before solving for the trajectory of the electron, let us first make some convenient notations

$$\tilde{p}_{x,y,z} = \frac{1}{m_e c}\gamma m_e v_{x,y,z} = \gamma\frac{v_{x,y,z}}{c}\,.$$

Thus the momenta can be written as

$$\tilde{\mathbf{p}} = \begin{pmatrix}\tilde{p}_x \\ \tilde{p}_y \\ \tilde{p}_z\end{pmatrix} = \begin{pmatrix}\gamma v_x/c \\ \gamma v_y/c \\ 0\end{pmatrix} = \begin{pmatrix}\frac{\gamma}{c}\frac{\mathrm{d}x}{\mathrm{d}t} \\ \frac{\gamma}{c}\frac{\mathrm{d}y}{\mathrm{d}t} \\ 0\end{pmatrix} = \frac{\gamma}{c}\frac{\mathrm{d}}{\mathrm{d}t}\begin{pmatrix}x \\ y \\ z\end{pmatrix}\,.$$

Since we have already found that the two constants of the motion are related to the momenta, we can use those to find the trajectory of the electron instead of directly solving equation (1.21)

$$\begin{pmatrix}\tilde{p}_x \\ \tilde{p}_y \\ \tilde{p}_z\end{pmatrix} = \begin{pmatrix}\frac{a^2}{2} \\ a \\ 0\end{pmatrix}\,.$$

To further simplify calculations, we can move to the frame of reference with $\tau = t - \frac{x(t)}{c}$. In this case

$$\gamma\frac{\mathrm{d}}{\mathrm{d}t} = \gamma\frac{\mathrm{d}\tau}{\mathrm{d}t}\frac{\mathrm{d}}{\mathrm{d}\tau} = \gamma\left(1 - \frac{1}{c}\frac{\mathrm{d}x}{\mathrm{d}t}\right)\frac{\mathrm{d}}{\mathrm{d}\tau} = \left(\gamma - \underbrace{\frac{\gamma}{c}\frac{\mathrm{d}x}{\mathrm{d}t}}_{\tilde{p}_x}\right)\frac{\mathrm{d}}{\mathrm{d}\tau} = (1 + \tilde{p}_x - \tilde{p}_x)\frac{\mathrm{d}}{\mathrm{d}\tau} = \frac{\mathrm{d}}{\mathrm{d}\tau}$$

and thus the system of equations to be solved will be given by

$$\begin{aligned}\frac{\mathrm{d}x}{\mathrm{d}\tau} &= c\frac{a^2}{2} \\ \frac{\mathrm{d}y}{\mathrm{d}\tau} &= ca \\ \frac{\mathrm{d}z}{\mathrm{d}\tau} &= 0\,.\end{aligned} \tag{1.28}$$

Since according to our notation

$$a = \frac{eA}{m_e c}\,,$$

we have

$$\begin{aligned}\mathbf{a} &= \frac{eA_0}{m_e c}\mathbf{e}_y\sin\phi = a_0\mathbf{e}_y\sin(kx - \omega t) \\ &= a_0\mathbf{e}_y\sin\left(kx - \omega\tau - \omega\frac{x(t)}{c}\right) \\ &= a_0\mathbf{e}_y\sin(-\omega\tau) \\ &= -a_0\mathbf{e}_y\sin(\omega\tau)\,,\end{aligned}$$

15

where we have used the fact that $k = \omega/c$.

Going now back to equation (1.28), we can integrate to find the trajectory of the electron. For the O_x component we have

$$x(\tau) = \frac{c}{2} \int a_0^2 \sin^2 \omega\tau \, \mathrm{d}\tau = \frac{ca_0^2}{2} \int \left(1 - \cos^2 \omega\tau\right) \mathrm{d}\tau = \frac{ca_0^2}{2} \int \frac{1 - \cos(2\omega\tau)}{2} \, \mathrm{d}\tau$$
$$= \frac{ca_0^2}{4} \left[\tau - \int \cos(2\omega\tau) \, \mathrm{d}\tau\right] = \frac{ca_0^2}{4} \left[\tau - \frac{1}{2\omega} \sin(2\omega\tau)\right] .$$

and for the O_y component

$$y(\tau) = -c \int a_0 \sin(\omega\tau) \, \mathrm{d}\tau = \frac{ca_0}{\omega} \left[1 - \cos(\omega\tau)\right] .$$

Thus, the motion of the electron in the selected frame of reference will be given by

$$x(\tau) = \frac{ca_0^2}{4} \left[\tau - \frac{1}{2\omega} \sin(2\omega\tau)\right]$$
$$y(\tau) = \frac{ca_0}{\omega} \left[1 - \cos(\omega\tau)\right]$$
$$z(\tau) = 0 .$$

The trajectory is a simple oscillation on the O_y direction, but more complex on the O_x direction. A plot illustrating the trajectory can be seen in figure 1.1. Taking a closer look at the motion on the O_x direction, we can see that it is a combination of a oscillation and a drift motion. The drift motion is given by

$$x = \frac{ca_0^2}{4}\tau = \frac{ca_0^2}{4}\left(t - \frac{x}{c}\right) = \frac{ca_0^2}{4}t - \frac{a_0^2}{4}x$$

or

$$x = \frac{ca_0^2}{4} \frac{t}{1 + \frac{a_0^2}{2}} = \frac{ca_0^2}{4 + a_0^2}t$$

with the drift velocity being given by

$$v_{drift} = \frac{ca_0^2}{4 + a_0^2}c$$

in the laboratory frame. If we follow the motion of the electron in a referance frame moving with the drift velocity, the motion of the electron will appear as a figure-8, as can be seen in figure 1.1.
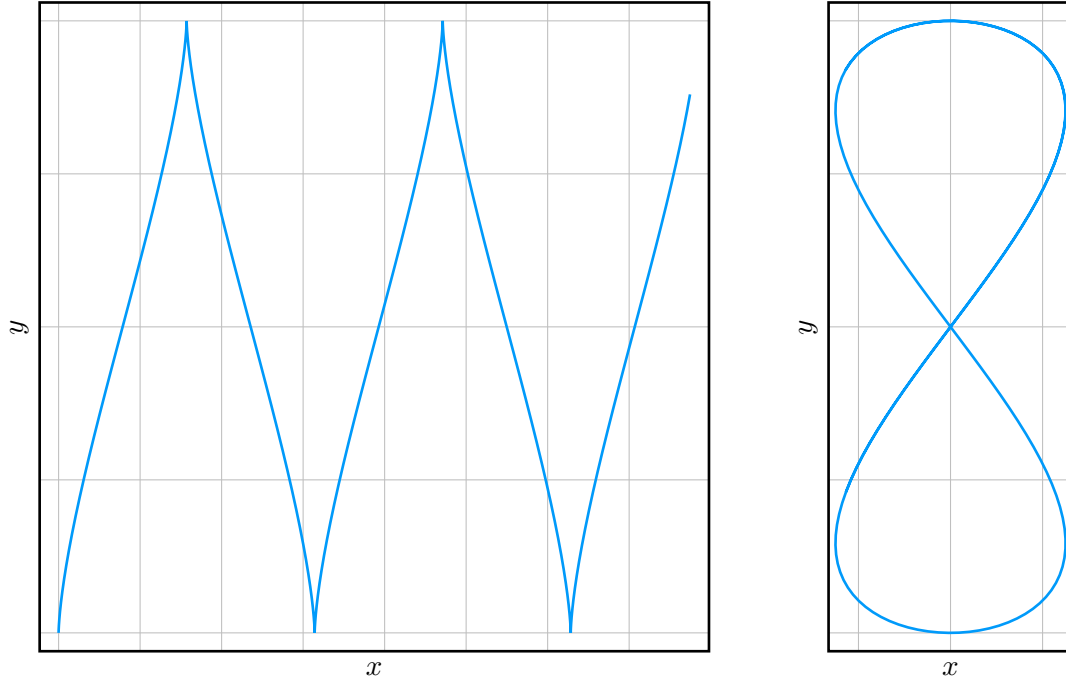
Figure 1.1: The trajectory of the electron in a plane wave in the laboratory frame (left) and in the average momentum frame (right)

1.5 The Ponderomotive Force

While the plane wave can be used as an approximation for a laser in some conditions, it cannot be used when the laser is focused and has a significant spatial variation. In the case of spatially varying fields, non-linear effects come into play and give rise to new physics. One such phenomena is the ponderomotive force that is excreted on charged particles in electromagnetic fields with non-vanishing gradient.

Qualitatively, this force can be seen as a radiation pressure that pushes charged particles away from the regions with high gradient. It is not an instantaneous effect, but an averaged one and thus charges will have a complicated motion, but on average they will be deflected due to this mechanism. One important aspect of this force is that it is independent of the sign of the charge. Thus, in a plasma, both electrons and nuclei are affected by this force, but since electrons are much lighter, they will be deflected far away from their equilibrium position.

We will begin with the derivation of the ponderomotive force in the non-relativistic case, but this effect can also be obtained in a covariant fashion.

1.5.1 Non-relativistic treatment

In order to treat the nonlinear effects induced by a spatially varying field, we will expand the electric field in a Taylor series. Assuming that the electric field is separable in a spatially varying part and a time dependent oscillation

$$\mathbf{E}(\mathbf{r}, t) = \mathbf{E}_s(\mathbf{r}) \cos(\omega t)\,,$$

then the spatial dependence of the electric field will be given by

$$\mathbf{E}_s(\mathbf{r}) = \mathbf{E}_s(\mathbf{r})\bigg|_{\mathbf{r}=\mathbf{r}_0} + \left(\Delta\mathbf{r}^{(1)} \cdot \boldsymbol{\nabla}\right) \mathbf{E}_s(\mathbf{r})\bigg|_{\mathbf{r}=\mathbf{r}_0} + \mathcal{O}(\Delta\mathbf{r}^2)$$

17

and the nonlinearity given by the magnetic field term can be expressed as a function of the electric field by integrating

$$\frac{\mathrm{d}\mathbf{B}}{\mathrm{d}t} = -\boldsymbol{\nabla} \times \mathbf{E}$$

and thus

$$\mathbf{B}^{(1)} = -\frac{1}{\omega}\boldsymbol{\nabla} \times \mathbf{E}\bigg|_{\mathbf{r}=\mathbf{r}_0} \sin(\omega t)\,,$$

where we have used $^{(\mathrm{n})}$ to denote the approximation order.

With these considerations, the nonlinear terms of the equation of motion yield

$$m_e\frac{\mathrm{d}\mathbf{v}^{(1)}}{\mathrm{d}t} = -e\left[\left(\Delta\mathbf{r}^{(1)} \cdot \boldsymbol{\nabla}\right)\mathbf{E}(\mathbf{r},t)\bigg|_{\mathbf{r}=\mathbf{r}_0} + \mathbf{v}^{(0)} \times \mathbf{B}^{(1)}\right]\,,$$

with the linear terms corresponding to

$$m_e\frac{\mathrm{d}\mathbf{v}^{(0)}}{\mathrm{d}t} = -e\mathbf{E}_s(\mathbf{r}_0)\cos(\omega t)\,.$$

Solving the equation for the linear part, we obtain

$$\mathbf{v}^{(0)} = -\frac{e}{m_e\omega}\mathbf{E}_s\sin(\omega t)$$

$$\Delta\mathbf{r}^{(1)} = \frac{e}{m_e\omega^2}\mathbf{E}_s\cos(\omega t)\,.$$

Replacing the results in the equation for the non-linear terms gives

$$m_e\frac{\mathrm{d}\mathbf{v}^{(1)}}{\mathrm{d}t} = -\frac{e^2}{m_e\omega^2}\left[(\mathbf{E}_s \cdot \boldsymbol{\nabla})\mathbf{E}_s(\mathbf{r},t)\bigg|_{\mathbf{r}=\mathbf{r}_0}\cos^2(\omega t) + \mathbf{E}_s \times (\boldsymbol{\nabla} \times \mathbf{E}_s)\sin^2(\omega t)\right]$$

Since the temporal and spatial parts are separated, we can get rid of the time dependent part by averaging over a period. Since the time dependent terms are either $\sin^2$ or $\cos^2$, when averaging over a period $T = 2\pi/\omega$

$$\left\langle m_e\frac{\mathrm{d}\mathbf{v}^{(1)}}{\mathrm{d}t}\right\rangle_T = \int_0^T m_e\frac{\mathrm{d}\mathbf{v}^{(1)}}{\mathrm{d}t}\,\mathrm{d}t\,,$$

we obtain a factor of $1/2$ because $\left\langle\sin^2(\omega t)\right\rangle_T = \left\langle\cos^2(\omega t)\right\rangle_T$ and $\sin^2(x) + \cos^2(x) = 1$.

Thus, we are left only with the spatial dependence

$$\left\langle m_e\frac{\mathrm{d}\mathbf{v}^{(1)}}{\mathrm{d}t}\right\rangle_T = -\frac{e^2}{2m_e\omega^2}\left[(\mathbf{E}_s \cdot \boldsymbol{\nabla})\mathbf{E}_s(\mathbf{r},t)\bigg|_{\mathbf{r}=\mathbf{r}_0} + \mathbf{E}_s \times (\boldsymbol{\nabla} \times \mathbf{E}_s)\right]\,. \tag{1.29}$$

The last term can be expanded into

$$\begin{aligned}
\mathbf{E}_s \times (\boldsymbol{\nabla} \times \mathbf{E}_s) &= \mathbf{e}_i\varepsilon_{ijk}E_j\varepsilon_{klm}\partial_l E_m\\
&= \mathbf{e}_i\left(\delta_{il}\delta_{jm} - \delta_{im}\delta_{jl}\right)E_j\partial_l E_m = \mathbf{e}_i\left(E_j\partial_i E_j - E_j\partial_j E_i\right)\\
&= \mathbf{E}_s \cdot \boldsymbol{\nabla}\mathbf{E}_s - (\mathbf{E}_s \cdot \boldsymbol{\nabla})\mathbf{E}_s\\
&= \frac{1}{2}\boldsymbol{\nabla}\left(\mathbf{E}_s^2\right) - (\mathbf{E}_s \cdot \boldsymbol{\nabla})\mathbf{E}_s\,,
\end{aligned}$$

where we have ommited the $_s$ subscript for the $\mathbf{E}_s$ vector components to simplify the notation. Using this reslt in equation (1.29) yields

$$\left\langle m_e\frac{\mathrm{d}\mathbf{v}^{(1)}}{\mathrm{d}t}\right\rangle_T = -\frac{e^2}{4m_e\omega^2}\boldsymbol{\nabla}\left(\mathbf{E}_s^2\right) \equiv \mathbf{F}_{pond} \tag{1.30}$$

the equation for the ponderomotive force.

1.5.2 Relativistic treatment

1.6 Laser Wakefield Acceleration

Chapter 2

Particle in Cell Method

As we outlined in Chapter 1, the interaction of some charged particles with an electromagnetic field can be viewed as the action of the sources on the fields and the action of the fields on the sources.

In the same manner, simulating the interaction self-consistently requires a *field solver* that computes the structure of the fields considering the sources and a *particle pusher* that solves the (relativistic) equations of motion for the particles. In the particle in cell method, a finite-difference time-domain (FDTD) method is used for solving Maxwell's equations and a modified leapfrog method is used for the particle pusher as presented in Arber *et al.* 2015.

2.1   Numerical Methods Introduction

The numerical methods mentioned above are based on the idea of discretising the derivative operator. There are multiple ways of discretising this operator, but all of them can be derived from the Taylor series expansion.

$$f(x_0 + h) = f(x_0) + \frac{f'(x_0)}{1!}h + \frac{f''(x_0)}{2!}h^2 + \cdots + \frac{f^{(n)}(x_0)}{n!}h^n + \cdots$$

The main discretisations options are the forward, backward and central differences. For the forward discretisation we consider

$$f(x_0 + h) = f(x_0) + \frac{f'(x_0)}{1!}h + \frac{f''(x_0)}{2!}h^2 + \cdots$$

and we rearrange the terms in the following way

$$\frac{f(x_0 + h) - f(x_0)}{h} = f'(x_0) + \frac{f''(x_0)}{2}h + \cdots$$

and thus, when $h \to 0$, the derivative in first order is given by

$$f'(x_0) = \frac{f(x_0 + h) - f(x_0)}{h} + \mathcal{O}(h) \, .$$

The local truncation error is given by the error of the approximation in one time step. The forward and backward discretisations are both of order one. The central discretisation is second order accurate and can be derived as follows.

We first begin with the forward and backward discretisations for half of a time step:

$$f(x_0 + \frac{h}{2}) = f(x_0) + f'(x_0)\frac{h}{2} + \frac{f''(x_0)}{2}\frac{h^2}{4} + \frac{f^{(3)}(x_0)}{3!}\frac{h^3}{8} + \cdots$$

$$f(x_0 - \frac{h}{2}) = f(x_0) - f'(x_0)\frac{h}{2} + \frac{f''(x_0)}{2}\frac{h^2}{4} - \frac{f^{(3)}(x_0)}{3!}\frac{h^3}{8} + \cdots .$$

Then we take the difference and obtain

$$f(x_0 + \frac{h}{2}) - f(x_0 - \frac{h}{2}) = f'(x_0)h + 2\frac{f^{(3)}(x_0)}{3!}\frac{h^3}{8} + \cdots$$

and we can see that indeed the central difference is second order accurate

$$f'(x_0) = \frac{f(x_0 + \frac{h}{2}) - f(x_0 - \frac{h}{2})}{h} + \mathcal{O}(h^2).$$

As an application of the methods discussed above, we will now derive the so called leapfrog method for solving second order differential equations following Hockney and Eastwood (1988, Chapter 4). More concretely, we will take a look at solving the equations of motion for a particle. As a first step, the equations of motion can be written as a system of first order differential equations

$$\frac{d\mathbf{x}}{dt} = \mathbf{v}$$

$$m\frac{d\mathbf{v}}{dt} = \mathbf{F},$$

where $\mathbf{F}$ is the total force on the particle. Replacing the derivatives with their finite difference approximations, we obtain

$$\frac{\mathbf{x}_{n+1} - \mathbf{x}_n}{\Delta t} = \mathbf{v}_{n+1/2} \tag{2.1a}$$

$$m\frac{\mathbf{v}_{n+1/2} - \mathbf{v}_{n-1/2}}{\Delta t} = \mathbf{F}(\mathbf{x}_n). \tag{2.1b}$$

Replacing the velocity, we obtain

$$\frac{\mathbf{x}_{n+1} - 2\mathbf{x}_n + \mathbf{x}_{n-1}}{\Delta t^2} = \frac{\mathbf{F}(\mathbf{x}_n)}{m}.$$

2.1.1 Accuracy

The accuracy of an integration method is given by difference between the true solution and the approximate solution at a given time step, that is the local error. There are two types of local errors: truncation errors and round-off errors. Truncation errors are given by the approximations employed in the numerical method. On the other hand, round-off errors are consequence of implementing the numerical method on a computer with finite precision. In general, for low order methods, the truncation errors are significantly bigger than round-off errors, and thus we can consider that the accuracy is given only by truncation error.

In order to better illustrate the concept of truncation errors, we will exemplify its computation for the leapfrog method. Let us consider the local truncation error at the time step n, δ^n and $\mathbf{X}$ the true solution

$$\frac{\mathbf{X}_{n+1} - 2\mathbf{X}_n + \mathbf{X}_{n-1}}{\Delta t^2} = \frac{\mathbf{F}(\mathbf{X}_n)}{m} + \delta^n.$$

If we expand $\mathbf{X}_{n+1}$ and $\mathbf{X}_{n-1}$ in Taylor series around $\mathbf{X}_n$

$$\mathbf{X}_{n+1} = \mathbf{X}_n + \frac{\mathrm{d}\mathbf{X}_n}{\mathrm{d}t}\Delta t + \frac{1}{2}\frac{\mathrm{d}^2\mathbf{X}_n}{\mathrm{d}t^2} - \cdots$$

$$\mathbf{X}_{n-1} = \mathbf{X}_n - \frac{\mathrm{d}\mathbf{X}_n}{\mathrm{d}t}\Delta t + \frac{1}{2}\frac{\mathrm{d}^2\mathbf{X}_n}{\mathrm{d}t^2} - \cdots,$$

we obtain

$$\frac{\mathrm{d}^2\mathbf{X}_n}{\mathrm{d}t^2} + \frac{\Delta t^2}{12}\frac{\mathrm{d}^4\mathbf{X}}{\mathrm{d}t^4} + \mathcal{O}\left(\Delta t^5\right) = \frac{\mathbf{F}(\mathbf{X}_n)}{m} + \delta^n,$$

and thus

$$\delta^n \sim \mathcal{O}\left(\Delta t^2\right)$$

which shows that the leapfrog algorithm is of order 2.

2.1.2 Stability

A numerical method is considered asymptotically stable if the solution obtained for a linear problem is asymptotically bounded. As in the previous case we will show an example for the leapfrog method, following the ideas exposed in Butcher 2016 and in Leimkuhler and Reich (2004, Section 2.6).

A linear problem can be written as

$$\frac{\mathrm{d}}{\mathrm{d}t}\mathbf{z} = A\mathbf{z},$$

where we used the following notation to denote the dynamical state of the system

$$\mathbf{z} = \begin{pmatrix} \mathbf{q} \\ \mathbf{p} \end{pmatrix}.$$

The solution can be written as

$$\mathbf{z}(t) = R(t)\mathbf{z}_0,$$

where $R(t)$ is a matrix which can give the solution at any time by evolving the initial conditions.

The discrete version of the problem is given by

$$\mathbf{z}_{n+1} = \hat{R}(\Delta t)\mathbf{z}_n, \tag{2.2}$$

where $\hat{R}(\Delta t)$ is called the propagation matrix. With this considerations, asymptotic stability can be expressed as a function of the eigenvalues of $\hat{R}(\Delta t)$, since the solution is obtained with powers of $\hat{R}$ from the initial conditions

$$\mathbf{z}_n = [\hat{R}]^n \mathbf{z}_0.$$

More concretely, a method is asymptotically stable if the eigenvalues of $\hat{R}$ are inside the unit disk in the complex plane and simple (not repeated) if on the unit circle (Leimkuhler and Reich 2004, p. 28).

One of the most studied linear problems is the harmonic oscillator and we can use it as our model linear problem

$$\mathcal{H} = \frac{\mathbf{p}^2}{2m} + \frac{\omega^2\mathbf{q}^2}{2}.$$

The equations of motion are given by the corresponding Hamilton equations

$$\dot{q}_i = \frac{\partial \mathcal{H}}{\partial p_i} = \frac{p_i}{m}$$

$$\dot{p}_i = -\frac{\partial \mathcal{H}}{\partial q_i} = -\omega^2 q_i \,.$$

Taking $m = 1$ and writing the above equations in matrix form yields

$$\dot{\mathbf{z}} = \begin{pmatrix} p \\ -\omega^2 q \end{pmatrix} = \begin{pmatrix} 0 & 1 \\ -\omega^2 & 0 \end{pmatrix} \begin{pmatrix} \mathbf{q} \\ \mathbf{p} \end{pmatrix}$$

and thus we obtain

$$\dot{\mathbf{z}} = A\mathbf{z},$$

with

$$A = \begin{pmatrix} 0 & 1 \\ -\omega^2 & 0 \end{pmatrix} \,.$$

The solution is given by

$$\mathbf{z}(t) = R(t)\mathbf{z}_0,$$

with

$$R(t) = \begin{pmatrix} \cos(\omega t) & \frac{1}{\omega}\sin(\omega t) \\ -\omega\sin(\omega t) & \cos(\omega t) \end{pmatrix} \,.$$

In order to analyse the stability of the leapfrog algorithm, it is convenient to express the equations in a different form, also called the Störmer–Verlet method

$$\mathbf{q}_{n+1} = \mathbf{q}_n + \Delta t \mathbf{v}_{n+1/2}$$

$$M\mathbf{v}_{n+1/2} = M\mathbf{v}_n - \frac{\Delta t}{2}\boldsymbol{\nabla}V(\mathbf{q}_n)$$

$$M\mathbf{v}_{n+1} = M\mathbf{v}_{n+1/2} - \frac{\Delta t}{2}\boldsymbol{\nabla}V(\mathbf{q}_{n+1}) \,.$$

In our particular case, the gradient of the potential is given by $\omega^2 q$ and the above reduces to

$$\mathbf{q}_{n+1} = \mathbf{q}_n + \Delta t(\mathbf{v}_n - \frac{\Delta t}{2}\omega^2 \mathbf{q}^n) = \mathbf{q}_n\left(1 - \frac{\Delta t^2 \omega^2}{2}\right) + \mathbf{v}_n \Delta t$$

$$\mathbf{p}_{n+1} = \mathbf{p}_n - \frac{\Delta t^2}{2}\omega^2 \mathbf{q}_n - \frac{\Delta t^2}{2}\omega^2 \mathbf{q}_{n+1} = \mathbf{p}_n - \frac{\Delta t^2}{2}\omega^2 \mathbf{q}_n - \frac{\Delta t}{2}\omega^2\left(\mathbf{q}_n + \mathbf{v}_n - \frac{\Delta t}{2}\omega^2 \mathbf{q}_n\right) \,,$$

or

$$\begin{pmatrix} \mathbf{q}_{n+1} \\ \mathbf{p}_{n+1} \end{pmatrix} = \begin{pmatrix} 1 - \frac{\Delta t^2 \omega^2}{2} & \Delta t \\ -\Delta t \omega^2\left(1 - \frac{\Delta t^2 \omega^2}{4}\right) & 1 - \frac{\Delta t^2 \omega^2}{2} \end{pmatrix} \begin{pmatrix} \mathbf{q}_n \\ \mathbf{p}_n \end{pmatrix} \,.$$

Comparing with equation (2.2) we obtain

$$\hat{R}(\Delta t) = \begin{pmatrix} 1 - \frac{\Delta t^2 \omega^2}{2} & \Delta t \\ -\Delta t \omega^2\left(1 - \frac{\Delta t^2 \omega^2}{4}\right) & 1 - \frac{\Delta t^2 \omega^2}{2} \end{pmatrix} \,.$$

The eigenvalues of $\hat{R}$ are given by the solution of $\det\left(\hat{R} - \lambda I\right) = 0$, or more explicitly

$$\begin{vmatrix} 1 - \frac{\Delta t^2 \omega^2}{2} & \Delta t \\ -\Delta t \omega^2\left(1 - \frac{\Delta t^2 \omega^2}{4}\right) & 1 - \frac{\Delta t^2 \omega^2}{2} \end{vmatrix} = 0 \,.$$

This reduces to

$$\left(1 - \frac{\Delta t^2 \omega^2}{2} - \lambda\right)^2 + \frac{\Delta t^2 \omega^2}{2}\left(2 - \frac{\Delta t^2 \omega^2}{2}\right) = 0\,.$$

Using the notation $\frac{\Delta t^2 w^2}{2} \equiv \mu^2$, we obtain

$$\left(1 - \mu^2 - \lambda\right)^2 + \mu^2\left(2 - \mu^2\right) = 0\,,$$

which can be further expanded to

$$\lambda^2 + \left(1 - \mu^2\right)^2 - 2\left(1 - \mu^2\right)\lambda + \mu^2\left(2 - \mu^2\right) = 0\,,$$

yielding the solutions

$$\lambda_{1,2} = \frac{1}{2}\left\{2(1-\mu^2) \pm \sqrt{4(1-\mu^2)^2 - 4\left[(1-\mu^2)^2 + \mu^2(2-\mu^2)\right]}\right\}$$
$$= 1 - \mu^2 \pm \sqrt{\mu^2(\mu^2 - 2)}\,.$$

We notice that for $\mu^2 < 2$ the solutions are complex and

$$|\lambda_{1,2}|^2 = (1 - \mu^2) + \mu^2(\mu^2 - 2)$$
$$= 1 + \mu^4 - 2\mu^2 + \mu^4 - 2\mu^2$$
$$= 1 + \mu^4 - 4\mu^2\,.$$

The method will be stable for $|\lambda|^2 < 1$, or

$$\mu^2(\mu^2 - 4) < 0 \implies \mu < 2, \text{for } \mu \neq 0\,.$$

For $\mu^2 > 2$ the eigenvalues are real and with modulus greater than 1. Thus the stability condition for the Störmer–Verlet method is given by $\mu < 2$, or

$$\Delta t^2 \omega^2 < 4\,,$$

indicating a sampling of at least π points per period, or a step size $\Delta t < 2/\omega$.

In the context of ordinary differential equations, a stability region of the method is usually defined via a stability function $R(z)$ in the complex plane (Butcher 2016, p. 81). Such approach cannot be used in this case since the stability function is defined for a singe ordinary differential equation, but in the case of Hamiltonian dynamics we always have $2n$ ordinary differential equations, with $n > 1$.

2.2   The particle pusher

Having (briefly) developed some general aspects of the theory of numerical methods for solving differential equations, we now continue with the more concrete case of numerically solving the equations of motion for a charged particle. In the non-relativistic case, the (continuous) equations of motion have the following form

$$\frac{\mathrm{d}\mathbf{x}}{\mathrm{d}t} = \mathbf{v}$$
$$\frac{\mathrm{d}\mathbf{v}}{\mathrm{d}t} = \frac{q}{m}\left(\mathbf{E} + \mathbf{v} \times \mathbf{B}\right)\,.$$

Since the above equations are symmetric with respect to time reversal, it is desired that we obtain a discretisation which is also time-reversible. Buneman (1967) explained that we can use centred differences for this task and in the particular case of the Lorentz force we can average the velocity in order to represent the $\mathbf{v} \times \mathbf{B}$ product symmetrically. Thus we obtain

$$\frac{\mathbf{x}_{n+1} - \mathbf{x}_n}{\Delta t} = \mathbf{v}_{n+1} \tag{2.3a}$$

$$\frac{\mathbf{v}_{n+1/2} - \mathbf{v}_{n-1/2}}{\Delta t} = \frac{q}{m} \left(\mathbf{E}(\mathbf{x}_n) + \frac{\mathbf{v}_{n+1/2} + \mathbf{v}_{n-1/2}}{2} \times \mathbf{B}(\mathbf{x}_n) \right) . \tag{2.3b}$$

As explained in Birdsall and Langdon (2005, Chapter 4–3), there are several methods for solving the above equations, implying a partial (Buneman 1967) or complete (Boris 1970) separation of the electric and magnetic force contributions. In the following we will detail the second method, which is also called the Boris push.

Let us introduce the following notation

$$\mathbf{v}^- = \mathbf{v}_{n-1/2} - \frac{q\mathbf{E}}{m} \frac{\Delta t}{2}$$

$$\mathbf{v}^+ = \mathbf{v}_{n+1/2} + \frac{q\mathbf{E}}{m} \frac{\Delta t}{2} ,$$

such that

$$\frac{\mathbf{v}^+ - \mathbf{v}^-}{\Delta t} = \frac{\mathbf{v}_{n+1/2} - \mathbf{v}_{n-1/2}}{\Delta t} + \frac{q\mathbf{E}}{m} .$$

Substituting in equation (2.3b) we obtain

$$\frac{\mathbf{v}^+ - \mathbf{v}^-}{\Delta t} = \frac{q}{2m}(\mathbf{v}^+ + \mathbf{v}^-) \times \mathbf{B} , \tag{2.4}$$

which can be seen as a rotation. Indeed, if we take the scalar product with $(\mathbf{v}^+ + \mathbf{v}^-)$, we get

$$(\mathbf{v}^+ + \mathbf{v}^-) \cdot \frac{\mathbf{v}^+ - \mathbf{v}^-}{\Delta t} = \frac{q}{2m} \underbrace{(\mathbf{v}^+ + \mathbf{v}^-) \cdot (\mathbf{v}^+ + \mathbf{v}^-) \times \mathbf{B}}_{0}$$

or

$$|\mathbf{v}^+|^2 - |\mathbf{v}^-|^2 = 0 ,$$

implying that $|\mathbf{v}^+| = |\mathbf{v}^-|$.

If we decompose the $\mathbf{v}^-$ into its parallel and perpendicular components with respect to $\mathbf{B}$, we can reduce the rotation of $\mathbf{v}^-$ to the rotation of its perpendicular component $\mathbf{v}_\perp^-$.

The angle of rotation between $\mathbf{v}_\perp^-$ and $\mathbf{v}_\perp^-$, denoted with θ in figure 2.1, can be expressed as

$$\tan \frac{\theta}{2} = \frac{|\mathbf{v}_\perp^+ - \mathbf{v}_\perp^-|}{|\mathbf{v}_\perp^+ + \mathbf{v}_\perp^-|} .$$

Rewriting equation (2.4) we obtain

$$\mathbf{v}^+ - \mathbf{v}^- = \frac{q\Delta t}{2m}(\mathbf{v}^+ + \mathbf{v}^-) \times \mathbf{B}$$

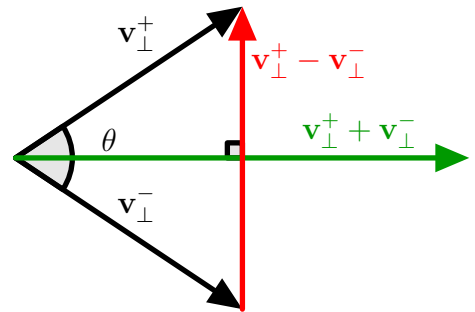and if we substitute $\mathbf{v}^\pm = \mathbf{v}_\perp^\pm + \mathbf{v}_\parallel^\pm$

Figure 2.1: Boris rotation angle

$$\mathbf{v}_\perp^+ - \mathbf{v}_\perp^- = \frac{q\Delta t}{2m}(\mathbf{v}_\perp^+ + \mathbf{v}_\perp^-) \times \mathbf{B} .$$

Furthermore, since all the vectors above have the same direction by construction, we can factor out the versors and obtain

$$\frac{|\mathbf{v}_\perp^+ - \mathbf{v}_\perp^-|}{|\mathbf{v}_\perp^+ + \mathbf{v}_\perp^-|} = \frac{q|\mathbf{B}|}{m}\frac{\Delta t}{2}$$

and thus

$$\tan\frac{\theta}{2} = \frac{qB}{m}\frac{\Delta t}{2}.$$ (2.5)

Since for the rotation described above only the components perpendicular to the direction of $\mathbf{B}$ matter, we can simplify the notation and use $\mathbf{v}_\pm$ instead of $\mathbf{v}_\perp^\pm$. We will now introduce an additional vector $\mathbf{v}'$ given by the addition between $\mathbf{v}_-$ and another vector, such that $\mathbf{v}'$ is perpendicular to $\mathbf{v}_+ - \mathbf{v}_-$.

It is convenient to write $\mathbf{v}'$ as $\mathbf{v}' = \mathbf{v}_- + \mathbf{v}_- \times \mathbf{t}$. In the right triangle formed by $\mathbf{v}'$ with $\mathbf{v}_-$ and $\mathbf{v}_- \times \mathbf{t}$ as seen in figure 2.2, we have

$$\tan\frac{\theta}{2} = \frac{|\mathbf{v}_- \times \mathbf{t}|}{|\mathbf{v}_-|} = |\mathbf{t}|$$

and thus by using equation (2.5) $\mathbf{t}$ is given by

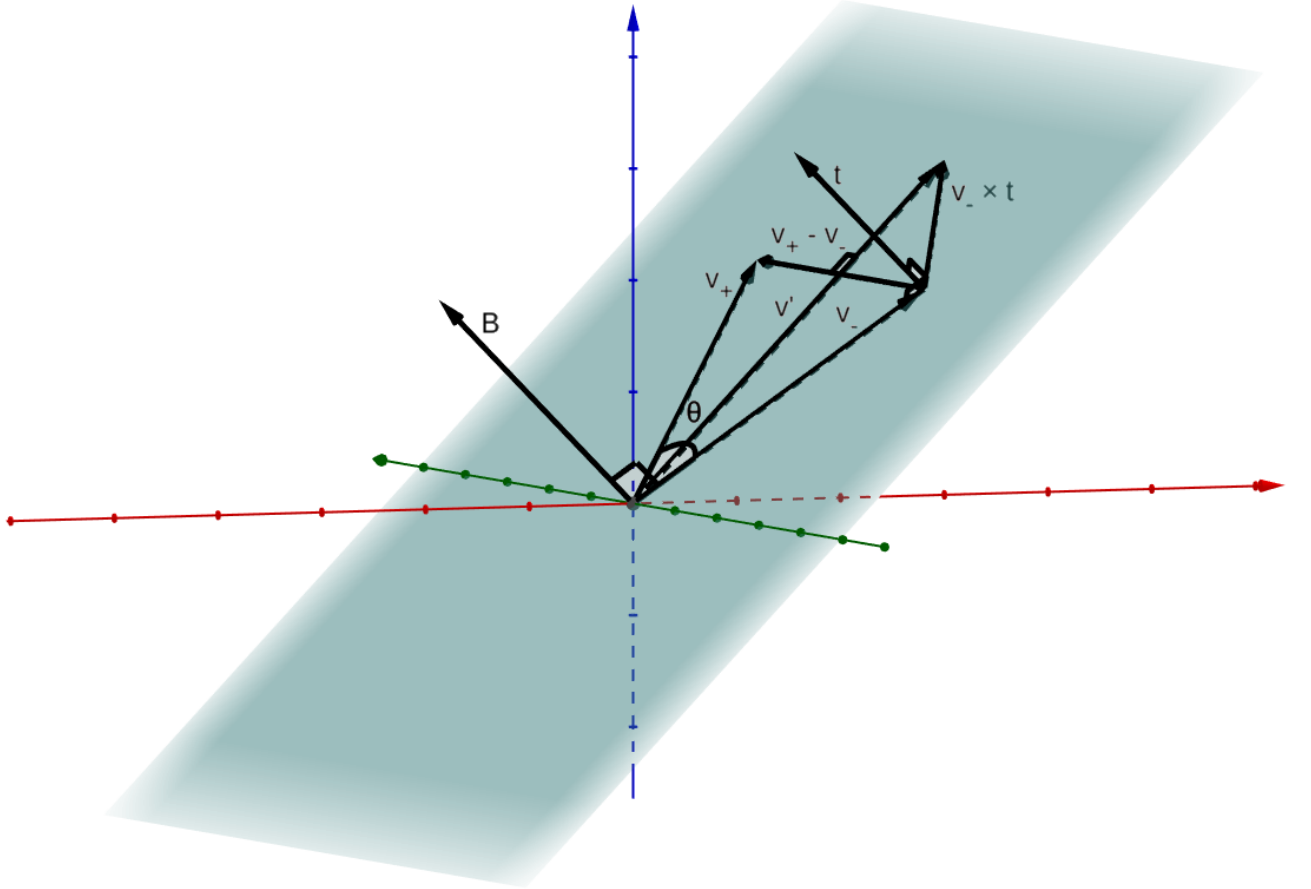$$\mathbf{t} = \frac{q\mathbf{B}}{m}\frac{\Delta t}{2}.$$

Figure 2.2: Boris rotation construction in 3D

As can be seen in figure 2.2, $\mathbf{v}_+ - \mathbf{v}_- \parallel \mathbf{v}' \times \mathbf{B}$. This encourages the following notation: $\mathbf{v}_+ - \mathbf{v}_- \equiv \mathbf{v}' \times \mathbf{s}$, where $\mathbf{s}$ can be determined by the condition that $|\mathbf{v}_+|^2 = |\mathbf{v}_-|^2$. Thus, expanding $\mathbf{v}' \times \mathbf{s}$ gives

$$\mathbf{v}' \times \mathbf{s} = (\mathbf{v}_- + \mathbf{v}_- \times \mathbf{t}) \times \mathbf{s} = \mathbf{v}_- \times \mathbf{s} + \mathbf{t}\underbrace{(\mathbf{v}_- \cdot \mathbf{s})}_{0} - \mathbf{v}_-(\mathbf{t} \cdot \mathbf{s})$$

and if we consider the definition for $\mathbf{s}$

$$\mathbf{v}_+ = \mathbf{v}_- + \mathbf{v}' \times \mathbf{s} = \mathbf{v}_- + \mathbf{v}_- \times \mathbf{s} - \mathbf{v}_-(\mathbf{t} \cdot \mathbf{s}).$$

Taking the scalar product with $\mathbf{v}_-$ gives

$$\mathbf{v}_+ \cdot \mathbf{v}_- = |\mathbf{v}_-|^2 - |\mathbf{v}_-|^2(\mathbf{t} \cdot \mathbf{s})$$

or

$$|\mathbf{v}_-|^2 \cos\theta = |\mathbf{v}_-|^2(1 - \mathbf{t} \cdot \mathbf{s}).$$

Using the trigonometry identity

$$\cos\theta = \frac{1 - \tan^2\frac{\theta}{2}}{1 + \tan^2\frac{\theta}{2}},$$

we obtain

$$\mathbf{t} \cdot \mathbf{s} = 1 - \frac{1 - \tan^2\frac{\theta}{2}}{1 + \tan^2\frac{\theta}{2}},$$

which is equivalent to

$$\mathbf{t} \cdot \mathbf{s} = \frac{2t^2}{1 + t^2}$$

and thus we obtain that

$$\mathbf{s} = \frac{2\mathbf{t}}{1 + t^2}.$$

Figure 2.3: The velocities projected in the plane perpendicular to $\mathbf{B}$

As a summary, the Boris push algorithm solves equation (2.3b) with the following steps:

1. $\mathbf{v}^- = \mathbf{v}_{n-1/2} + \frac{q\mathbf{E}}{m}\frac{\Delta t}{2}$

2. rotate $\mathbf{v}^-$ to obtain $\mathbf{v}^+$ using

   (a) $\mathbf{v}' = \mathbf{v}^- + \mathbf{v}^- \times \mathbf{t}$, where $\mathbf{t} = \frac{q\mathbf{B}}{m}\frac{\Delta t}{2}$
   (b) $\mathbf{v}^+ = \mathbf{v}^- + \mathbf{v}' \times \mathbf{s}$, where $\mathbf{s} = \frac{2\mathbf{t}}{1+t^2}$

3. $\mathbf{v}_{n+1/2} = \mathbf{v}^+ + \frac{q\mathbf{E}}{m}\frac{\Delta t}{2}$

2.2.1 Conservation properties

When solving (continuous) differential equations with (discrete) numerical methods, an important aspect is that we want the algorithm to be as close as possible to the original continuous system in terms of symmetries and conserved quantities (Stuart and Humphries 1996).

In what follows we will look at the conservation properties of the Boris push and show why are they important for simulating the dynamics of charged particles following the ideas presented in Qin et al. (2013).
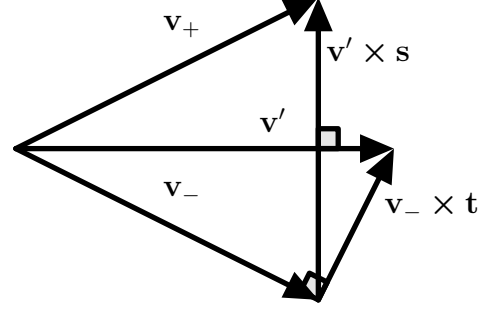
Mathematically speaking, a Hamiltonian system is given by the phase space (an even dimensional manifold[1]), a symplectic structure on it and the Hamiltonian function (Arnol'd 1989, p. 160). In order to explain what the symplectic structure is, we will start with a short discussion about 2-forms (Arnol'd 1989, p. 164).

Definition. An exterior form of degree 2 (or a 2-form) is a function of pairs of vectors $\omega^2 :$ $\mathbb{R}^n \times \mathbb{R}^n$, which is bilinear and skew symmetric:

$$\omega^2(\lambda_1 \boldsymbol{\xi}_1 + \lambda_2 \boldsymbol{\xi}_2, \boldsymbol{\xi}_3) = \lambda_1 \omega^2(\boldsymbol{\xi}_1, \boldsymbol{\xi}_3) + \lambda_2 \omega^2(\boldsymbol{\xi}_2, \boldsymbol{\xi}_3)$$
$$\omega^2(\boldsymbol{\xi}_1, \boldsymbol{\xi}_2) = -\omega^2(\boldsymbol{\xi}_2, \boldsymbol{\xi}_1) \,,$$

$\forall \lambda_{1,2} \in \mathbb{R}, \boldsymbol{\xi}_{1,2,3} \in \mathbb{R}^n$.

As an example of a 2-form in $n = 2$ dimensions is given by the *oriented area* spanned by 2 vectors in the (oriented) euclidean plane $\mathbb{R}^2$. Let us consider

$$\boldsymbol{\xi} = \begin{pmatrix} \xi_1 \\ \xi_2 \end{pmatrix}, \qquad \boldsymbol{\eta} = \begin{pmatrix} \eta_1 \\ \eta_2 \end{pmatrix},$$

then the oriented are determined by the two vectors is given by the determinant (Golomb 1985)

$$S(\boldsymbol{\xi}, \boldsymbol{\eta}) = \det \begin{pmatrix} \xi_1 & \eta_1 \\ \xi_2 & \eta_2 \end{pmatrix} = \xi_1 \eta_2 - \xi_2 \eta_1 \,.$$

Let us consider an $2d$-dimensional phase space with the coordinates q_i, p_i as presented in Leimkuhler and Reich (2004, p. 183).

Definition 1. A linear map $A : \mathbb{R}^{2d} \to \mathbb{R}^{2d}$ is called *symplectic* if there exists a 2-form ω such that

$$\omega(A\boldsymbol{\xi}, A\boldsymbol{\eta}) = \omega(\boldsymbol{\xi}, \boldsymbol{\eta}) \,, \ \forall \boldsymbol{\xi}, \boldsymbol{\eta} \in \mathbb{R}^{2d} \,.$$

We can also express the above in matrix notation

$$A^T J^{-1} A = J^{-1}, \qquad \text{where } J = \begin{pmatrix} 0 & I \\ -I & 0 \end{pmatrix},$$

with I the identity matrix in d dimensions.

A useful example that illustrates the concept is given in the case of $d = 1$, where symplecticity implies area conservation under the given linear transformation. In the more general $d > 1$ case, it would imply the conservation of the sum of the respective projected areas.

As we have seen from the beginning of this chapter, differentiable functions are often approximated using linear maps. This provides the motivation for extending the above definition to the non-linear case.

Definition 2. A differentiable map $g : U \to \mathbb{R}^{2d}$, with $U \subset \mathbb{R}^{2d}$ an open set, is called *symplectic* if its corresponding Jacobian matrix $g'(\mathbf{p}, \mathbf{q})$ is everywhere symplectic, i.e.

$$\omega(g'(\mathbf{p}, \mathbf{q})\boldsymbol{\xi}, g'(\mathbf{p}, \mathbf{q})\boldsymbol{\eta}) = \omega(\boldsymbol{\xi}, \boldsymbol{\eta})$$

or in matrix notation $g'(\mathbf{p}, \mathbf{q})^T J^{-1} g'(\mathbf{p}, \mathbf{q}) = J^{-1}$.

---

[1]A manifold is a topological space that is locally Euclidean.

Having defined symplecticity, we will now try to check if the Boris push algorithm is symplectic. For this task we begin with rewriting equation (2.3b) in a more convenient form

$$\mathbf{v}_{n+1/2} - \frac{q\Delta t}{2m}\mathbf{v}_{n+1/2} \times \mathbf{B}_n = \mathbf{v}_{n-1/2} + \frac{q\Delta t}{2m}\mathbf{v}_{n-1/2} \times \mathbf{B}_n + \frac{q\Delta t}{m}\mathbf{E}_n \,,$$

where $\mathbf{B}_n \equiv \mathbf{B}(\mathbf{x}_n)$ and $\mathbf{E}_n \equiv \mathbf{E}(\mathbf{x}_n)$.

In order to manipulate the above more easily, it is useful to introduce some fundamental group theory notions (Hairer, Lubich, and Wanner 2006, p. 118) and the hat map (Marsden and Ratiu 1999, p. 289).

Definition 3. A *Lie group G* is a group that is also a differentiable manifold and for which the product is given by the differentiable mapping $G \times G \to G$.

The tangent space $\mathfrak{g} = T_I G$ at the identity I of a matrix Lie group G is closed under forming commutators of its elements and defines the *Lie algebra* of G.

Definition 4. The *hat map* $\hat{\ }: \mathbb{R}^3 \to \mathfrak{so}(3)$ is a vector space isomorphism that identifies the Lie algebra $\mathfrak{so}(3)$ of $SO(3)$ with $\mathbb{R}^3$. If we consider $\mathbf{v} = (v_1, v_2, v_3) \in \mathbb{R}^3$, then the hat map is given by

$$\hat{\mathbf{v}} = \begin{pmatrix} 0 & -v_3 & v_2 \\ v_3 & 0 & -v_1 \\ -v_2 & v_1 & 0 \end{pmatrix}.$$

We can observe that

$$\hat{\mathbf{v}}\mathbf{w} = \mathbf{v} \times \mathbf{w}$$

characterizes the isomorphism. Comparing

$$\hat{\mathbf{v}}\mathbf{w} = \begin{pmatrix} 0 & -v_3 & v_2 \\ v_3 & 0 & -v_1 \\ -v_2 & v_1 & 0 \end{pmatrix} \begin{pmatrix} w_1 \\ w_2 \\ w_3 \end{pmatrix} = \begin{pmatrix} -v_3 w_2 + v_2 w_3 \\ v_3 w_1 - v_1 w_3 \\ -v_2 w_1 + v_1 w_2 \end{pmatrix}$$

with

$$(\mathbf{v} \times \mathbf{w}) = \mathbf{e}_i \epsilon_{ijk} v_j w_k = \mathbf{e}_1 (v_2 w_3 - v_3 w_2) + \mathbf{e}_2 (v_3 w_1 - v_1 w_3) + \mathbf{e}_3 (v_1 w_2 - v_2 w_1)$$

we can see that this is indeed true.

Thus, if we consider $\mathbb{R}^3$ together with the cross product, the hat map $\hat{\ }$ becomes a Lie algebra isomorphism and we can identify $\mathfrak{so}(3)$ with $\mathbb{R}^3$ having the cross product as Lie bracket[2].

We can now resume rewriting equation (2.3b) and we obtain

$$\left(I - \hat{\Omega}_n\right) \begin{pmatrix} v^1_{n+1/2} \\ v^2_{n+1/2} \\ v^3_{n+1/2} \end{pmatrix} = \left(I + \hat{\Omega}_n\right) \begin{pmatrix} v^1_{n-1/2} \\ v^2_{n-1/2} \\ v^3_{n-1/2} \end{pmatrix} + \frac{q\Delta t}{m} \begin{pmatrix} E^1_n \\ E^2_n \\ E^3_n \end{pmatrix}, \qquad (2.6)$$

where

$$\hat{\Omega}_n = \frac{q\Delta t}{2m} \begin{pmatrix} 0 & -B^3_n & B^2_n \\ B^3_n & 0 & -B^1_n \\ -B^2_n & B^1_n & 0 \end{pmatrix}.$$

---

[2] A bilinear, skew symmetric operation $\mathfrak{g} \times \mathfrak{g} \to \mathfrak{g}$ that satisfies the Jacobi identity.

Multiplying on the left of equation (2.6) with $\left(I - \hat{\Omega}_n\right)$ yields

$$\begin{pmatrix} v^1_{n+1/2} \\ v^2_{n+1/2} \\ v^3_{n+1/2} \end{pmatrix} = \left(I - \hat{\Omega}_n\right)^{-1}\left(I + \hat{\Omega}_n\right)\begin{pmatrix} v^1_{n-1/2} \\ v^2_{n-1/2} \\ v^3_{n-1/2} \end{pmatrix} + \frac{q\Delta t}{m}\left(I - \hat{\Omega}_n\right)^{-1}\begin{pmatrix} E^1_n \\ E^2_n \\ E^3_n \end{pmatrix} .$$

In order to further simplify the notation, we can use the following notation: $\mathbf{x}_n \equiv \mathbf{x}_k$ and $\mathbf{v}_{n-1/2} \equiv \mathbf{v}_k$ and use the Cayley transform for the first term on the right hand side. For a quadratic Lie group[3], the *Cayley transform*

$$\mathrm{cay}\,\Omega = (I - \Omega)^{-1}(I + \Omega)$$

maps elements of $\mathfrak{g}$ into G (Hairer, Lubich, and Wanner 2006, p. 128).

In our particular case

$$\left(I - \hat{\Omega}_n\right)^{-1}\left(I + \hat{\Omega}_n\right) = \mathrm{cay}\,\hat{\Omega}_n \equiv R$$

and we obtain

$$\mathbf{v}_{k+1} = R\mathbf{v}_k + \frac{q\Delta t}{m}\left(I - \hat{\Omega}_n\right)^{-1}\mathbf{E}_k .$$

Thus equations (2.3a) and (2.3b) form a one step map Ψ_B which maps $\mathbf{z}_k \equiv (\mathbf{x}_k, \mathbf{v}_k)$ to $\mathbf{z}_{k+1} \equiv (\mathbf{x}_{k+1}, \mathbf{v}_{k+1})$

$$\Psi_B : \begin{cases} \mathbf{x}_{k+1} = \mathbf{x}_k + R\Delta t\mathbf{v}_k + \dfrac{q\Delta t}{m}\left(I - \hat{\Omega}_n\right)^{-1}\mathbf{E}_k \\[2mm] \mathbf{v}_{k+1} = R\mathbf{v}_k + \dfrac{q\Delta t^2}{m}\left(I - \hat{\Omega}_n\right)^{-1}\mathbf{E}_k \end{cases} .$$

As Ψ_B is a function $\Psi_B(\mathbf{z}_k)$, we can compute its Jacobian an check the condition for symplecticity

$$\frac{\partial \Psi_B}{\partial \mathbf{z}_k} = \begin{pmatrix} \frac{\partial \mathbf{x}_{k+1}}{\partial \mathbf{x}_k} & \frac{\partial \mathbf{x}_{k+1}}{\partial \mathbf{v}_k} \\ \frac{\partial \mathbf{v}_{k+1}}{\partial \mathbf{x}_k} & \frac{\partial \mathbf{v}_{k+1}}{\partial \mathbf{v}_k} \end{pmatrix} = \begin{pmatrix} I + \Delta t\frac{\partial \mathbf{v}_{k+1}}{\partial \mathbf{x}_k} & R\Delta t \\ \frac{\partial \mathbf{v}_{k+1}}{\partial \mathbf{x}_k} & R \end{pmatrix} .$$

As we mentioned in definition 2, for the map to be symplectic it has to satisfy

$$\left(\frac{\partial \Psi_B}{\partial \mathbf{z}_k}\right)^T J^{-1}\left(\frac{\partial \Psi_B}{\partial \mathbf{z}_k}\right) = J^{-1} .$$

Considering

$$\frac{\partial \Psi_B}{\partial \mathbf{z}_k} = \begin{pmatrix} S_1 & S_2 \\ S_3 & S_4 \end{pmatrix} ,$$

the symplecticity condition can be written as

$$\begin{pmatrix} S_1^T & S_3^T \\ S_2^T & S_4^T \end{pmatrix}\begin{pmatrix} 0 & -I \\ I & 0 \end{pmatrix}\begin{pmatrix} S_1 & S_2 \\ S_3 & S_4 \end{pmatrix} = \begin{pmatrix} S_3^T & -S_1^T \\ S_4^T & -S_2^T \end{pmatrix}\begin{pmatrix} S_1 & S_2 \\ S_3 & S_4 \end{pmatrix}$$
$$= \begin{pmatrix} S_3^T S_1 - S_1^T S_3 & S_3^T S_2 - S_1^T S_4 \\ S_4^T S_1 - S_2^T S_3 & S_4^T S_2 - S_2^T S_4 \end{pmatrix}$$
$$= \begin{pmatrix} 0 & -I \\ I & 0 \end{pmatrix} .$$

---

[3]Lie groups of the form $G = \{Y \,|\, Y^T P Y = P\}$, where P is a constant matrix.

Thus, we will have the following set of conditions

$$S_3^T S_1 = S_1^T S_3 \tag{2.7a}$$
$$S_1^T S_4 - S_3^T S_2 = I \tag{2.7b}$$
$$S_4^T S_1 - S_2^T S_3 = I \tag{2.7c}$$
$$S_4^T S_2 = S_2^T S_4 \,. \tag{2.7d}$$

If we consider the simplified case of homogeneous electric and magnetic fields, then

$$\frac{\partial \mathbf{v}_{k+1}}{\partial \mathbf{x}_k} = \frac{\partial}{\partial \mathbf{x}_k}(R\mathbf{v}_k) + \frac{q\Delta t}{m}\frac{\partial}{\partial \mathbf{x}_k}\left[\left(I - \hat{\Omega}_k\right)^{-1}\mathbf{E}_k\right] = 0$$

and

$$S_1 = I \quad S_2 = R\Delta t$$
$$S_3 = 0 \quad S_4 = R\,.$$

If we consider the condition in equation (2.7b), we obtain

$$S_1^T S_4 - S_3^T S_2 = R \neq I$$

and thus the Boris push algorithm is not symplectic. In spite of that, the algorithm presents desirable properties such as near-conservation of energy when the magnetic field is constant or the electric potential is quadratic and for more general cases it has a linear energy error (Hairer and Lubich 2018). This properties encourage a more detailed analysis of the properties of the Boris push method.

One of the properties of a symplectic algorithm is that it conserves the phase space volume. This can be understood as a generalization of the are conservation example in $2d, d = 1$ to higher dimensions. For a map to be volume preserving, the determinant of its Jacobian must be one

$$\det\frac{\partial \Psi_B}{\partial \mathbf{z}_k} = 1\,.$$

In our case this becomes

$$\left|\frac{\partial \Psi_B}{\partial \mathbf{z}_k}\right| = \begin{vmatrix} I + \Delta t\frac{\partial \mathbf{v}_{k+1}}{\partial \mathbf{x}_k} & R\Delta t \\ \frac{\partial \mathbf{v}_{k+1}}{\partial \mathbf{x}_k} & R \end{vmatrix} = \begin{vmatrix} I & 0 \\ \frac{\partial \mathbf{v}_{k+1}}{\partial \mathbf{x}_k} & R \end{vmatrix} = |R|\,,$$

where we have subtracted the second row multiplied by Δt from the first one. Since $R \in SO(3)$, as a property of the Cayley transform,

$$|R| = 1$$

and thus the Boris push is volume preserving.

2.2.2 Shape functions

2.2.3 The relativistic case

The Boris push algorithm also has a relativistic variant, which takes into account the γ factor. The relativistic version is also volume preserving (Higuera and Cary 2017).

2.3 The field solver

We now turn our attention to the electromagnetic field equations. In order to compute the time evolution of the fields, we will use the equations containing their time derivatives, namely

$$\frac{\partial \mathbf{B}}{\partial t} = -\boldsymbol{\nabla} \times \mathbf{E} \tag{2.8}$$

$$\frac{\partial \mathbf{E}}{\partial t} = c^2 \boldsymbol{\nabla} \times \mathbf{B} - \frac{1}{\varepsilon_0}\mathbf{j}. \tag{2.9}$$

Kane Yee (1966) proposed a method for solving Maxwell's equations in isotropic media involving a leapfrog-like algorithm, but with staggering also in space. In order to illustrate this more easily, we will begin with the one dimensional case

$$\frac{\partial B_y}{\partial t} = -\frac{\partial E_x}{\partial z}$$

$$\frac{\partial E_x}{\partial t} = -c^2\frac{\partial B_y}{\partial z} - \frac{1}{\varepsilon_0}j_x \,,$$

in which the equations are discretised as follows:

$$\frac{B_y^{n+1/2}(k+\frac{1}{2}) - B_y^{n-1/2}(k+\frac{1}{2})}{\Delta t} = -\frac{E_x^n(k+1) - E_x^n(k)}{\Delta z} \tag{2.10a}$$

$$\frac{E_x^{n+1}(k) - E_x^n(k)}{\Delta t} = -c^2\frac{B_y^{n+1/2}(k+\frac{1}{2}) - B_y^{n+1/2}(k-\frac{1}{2})}{\Delta z} - \frac{1}{\varepsilon_0}j_x^{n+1/2}(k)\,. \tag{2.10b}$$

Let us now take a closer look at these discretisations by comparing with the typical form of the leapfrog algorithm (2.1a). For the magnetic field in equation (2.10a), the time derivatives of the fields are computed using the $B^{n+1/2} - B^{n-1/2}$ difference with the source term at step n. At the same time, for the electric field, the $E(k+1) - E(k)$ difference is used and the source term is at $k + \frac{1}{2}$. Thus, the values for the electric field are taken at integer k and n, but for the magnetic field, we use the values at half-integer k and n, creating thus a staggering in both space and time. Moving on to equation (2.10b), the time derivative for the electric field uses the $E^{n+1} - E^n$ difference with the source term at $n + \frac{1}{2}$ and similarly the magnetic field has the spatial derivative using the $B(k+\frac{1}{2}) - B(k-\frac{1}{2})$ difference with the source term at k. This swap in the steps used by the derivatives can be explained by the fact that in both equations we are observing the field at the same (space-time) points.

We can now generalize equations (2.10) to the 3-dimensional case. In this case Faraday's law in equation (2.8) becomes

$$\frac{\partial B_x}{\partial t} = -\frac{\partial E_z}{\partial y} + \frac{\partial E_y}{\partial z}$$

$$\frac{\partial B_y}{\partial t} = -\frac{\partial E_x}{\partial z} + \frac{\partial E_z}{\partial x}$$

$$\frac{\partial B_z}{\partial t} = -\frac{\partial E_y}{\partial x} + \frac{\partial E_x}{\partial y} \,.$$

To better emphasize the differences from equation (2.10a), we will focus on the O_y components. Thus the discrete form will be given by

$$\frac{B_y^{n+1/2}(i+\frac{1}{2}, j, k+\frac{1}{2}) - B_y^{n-1/2}(i+\frac{1}{2}, j, k+\frac{1}{2})}{\Delta t} =$$
$$-\frac{E_x^n(i+\frac{1}{2}, j, k+1) - E_x^n(i+\frac{1}{2}, j, k)}{\Delta z} + \frac{E_z^n(i+1, j, k+\frac{1}{2}) - E_z^n(i, j, k+\frac{1}{2})}{\Delta x} \,. \tag{2.11}$$

Since it is quite tedious to write everything explicitly, several shorthand notations have been developed. For example, Lehe (2018 15–26 January[a]) uses

$$F_{i,j,k}^n \equiv F^n(i,j,k)$$

and

$$\partial_t F|_{i,j,k}^n \equiv \frac{F_{i,j,k}^{n+\frac{1}{2}} - F_{i,j,k}^{n-\frac{1}{2}}}{\Delta t} \qquad \partial_x F|_{i,j,k}^n \equiv \frac{F_{i+\frac{1}{2},j,k}^n - F_{i-\frac{1}{2},j,k}^n}{\Delta x}$$

$$\partial_y F|_{i,j,k}^n \equiv \frac{F_{i,j+\frac{1}{2},k}^n - F_{i,j-\frac{1}{2},k}^n}{\Delta y} \qquad \partial_z F|_{i,j,k}^n \equiv \frac{F_{i,j,k+\frac{1}{2}}^n - F_{i,j,k-\frac{1}{2}}^n}{\Delta z}\,.$$

With these notations, equation (2.11) becomes

$$\partial_t B_y|_{i+\frac{1}{2},j,k+\frac{1}{2}}^n = -\partial_z E_x|_{i+\frac{1}{2},j,k+\frac{1}{2}}^n + \partial_x E_z|_{i+\frac{1}{2},j,k+\frac{1}{2}}^n$$

and by applying the same for the rest of the components we obtain

$$\partial_t B_x|_{i,j+\frac{1}{2},k+\frac{1}{2}}^n = -\partial_y E_z|_{i,j+\frac{1}{2},k+\frac{1}{2}}^n + \partial_z E_y|_{i+\frac{1}{2},j,k+\frac{1}{2}}^n$$

$$\partial_t B_y|_{i+\frac{1}{2},j,k+\frac{1}{2}}^n = -\partial_z E_x|_{i+\frac{1}{2},j,k+\frac{1}{2}}^n + \partial_x E_z|_{i+\frac{1}{2},j,k+\frac{1}{2}}^n$$

$$\partial_t B_z|_{i+\frac{1}{2},j,k+\frac{1}{2}}^n = -\partial_x E_y|_{i+\frac{1}{2},j+\frac{1}{2},k}^n + \partial_y E_x|_{i+\frac{1}{2},j+\frac{1}{2},k}^n\,.$$

In a similar fashion, Ampère's law in equation (2.9) becomes

$$\frac{\partial E_x}{\partial t} = -c^2\frac{\partial B_y}{\partial z} + c^2\frac{\partial B_z}{\partial y} - \frac{1}{\varepsilon_0}j_x$$

$$\frac{\partial E_y}{\partial t} = -c^2\frac{\partial B_z}{\partial x} + c^2\frac{\partial B_x}{\partial z} - \frac{1}{\varepsilon_0}j_y$$

$$\frac{\partial E_z}{\partial t} = -c^2\frac{\partial B_x}{\partial y} + c^2\frac{\partial B_y}{\partial x} - \frac{1}{\varepsilon_0}j_z$$

and the analogue of equation (2.10b) for the Ox axis will be

$$\frac{E_x^{n+1}(i+\frac{1}{2},j,k) - E_x^n(i+\frac{1}{2},j,k)}{\Delta t} = -c^2\frac{B_y^{n+1/2}(i+\frac{1}{2},j,k+\frac{1}{2}) - B_y^{n+1/2}(i+\frac{1}{2},j,k-\frac{1}{2})}{\Delta z}$$

$$+c^2\frac{B_z^{n+1/2}(i+\frac{1}{2},j+\frac{1}{2},k) - B_z^{n+1/2}(i+\frac{1}{2},j-\frac{1}{2},k)}{\Delta x} - \frac{1}{\varepsilon_0}j_x^{n+1/2}\,.$$

$$(2.12)$$

Using the compact notation above, we obtain

$$\partial_t E_x|_{i+\frac{1}{2},j,k}^{n+\frac{1}{2}} = c^2\partial_y B_z|_{i+\frac{1}{2},j,k}^{n+\frac{1}{2}} - c^2\partial_z B_y|_{i+\frac{1}{2},j,k}^{n+\frac{1}{2}} - \frac{1}{\varepsilon_0}j_x|_{i+\frac{1}{2},j,k}^{n+\frac{1}{2}}$$

$$\partial_t E_y|_{i,j+\frac{1}{2},k}^{n+\frac{1}{2}} = c^2\partial_z B_x|_{i,j+\frac{1}{2},k}^{n+\frac{1}{2}} - c^2\partial_x B_z|_{i,j+\frac{1}{2},k}^{n+\frac{1}{2}} - \frac{1}{\varepsilon_0}j_y|_{i,j+\frac{1}{2},k}^{n+\frac{1}{2}}$$

$$\partial_t E_z|_{i,j,k+\frac{1}{2}}^{n+\frac{1}{2}} = c^2\partial_x B_y|_{i,j,k+\frac{1}{2}}^{n+\frac{1}{2}} - c^2\partial_y B_x|_{i,j,k+\frac{1}{2}}^{n+\frac{1}{2}} - \frac{1}{\varepsilon_0}j_z|_{i,j,k+\frac{1}{2}}^{n+\frac{1}{2}}\,.$$

We can observe that we have only used tow of the four Maxwell equations to describe the evolution of the fields, so we should check that the other two equations are satisfied. Let us begin with the divergence of the magnetic field

$$\boldsymbol{\nabla}\cdot\mathbf{B} = 0\,.$$

33

Assuming that the relation is initially valid and

$$\frac{\partial \mathbf{B}}{\partial t} = -\boldsymbol{\nabla} \times \mathbf{E}$$

is satisfied all the time, then

$$\frac{\partial \boldsymbol{\nabla} \cdot \mathbf{B}}{\partial t} = \boldsymbol{\nabla} \cdot \frac{\partial \mathbf{B}}{\partial t} = \boldsymbol{\nabla} \cdot (-\boldsymbol{\nabla} \times \mathbf{E}) = 0 \,.$$

The discretised equations thus satisfy $\boldsymbol{\nabla} \cdot \mathbf{B} = 0$ since the above equation vanishes by the cancellation of identical derivative terms. The discretised version of this condition can be written as

$$\partial_x B_x |_{i+\frac{1}{2},j+\frac{1}{2},k+\frac{1}{2}}^{n+\frac{1}{2}} + \partial_y B_y |_{i+\frac{1}{2},j+\frac{1}{2},k+\frac{1}{2}}^{n+\frac{1}{2}} + \partial_z B_z |_{i+\frac{1}{2},j+\frac{1}{2},k+\frac{1}{2}}^{n+\frac{1}{2}} = 0 \,.$$

We will now continue with the divergence of the electric field

$$\boldsymbol{\nabla} \cdot \mathbf{E} = \frac{\rho}{\varepsilon_0} \,.$$

Again, we suppose that the relation is satisfied initially and that

$$\frac{\partial \mathbf{E}}{\partial t} = c^2 \boldsymbol{\nabla} \times \mathbf{B} - \frac{1}{\varepsilon_0} \mathbf{j}$$

is valid all the time. Then

$$\frac{\partial}{\partial t} \left(\boldsymbol{\nabla} \cdot \mathbf{E} - \frac{\rho}{\varepsilon_0} \right) = -\frac{1}{\varepsilon_0} \left[\frac{\partial \rho}{\partial t} - \boldsymbol{\nabla} \cdot \left(\frac{1}{\mu_0} \boldsymbol{\nabla} \times \mathbf{B} - \mathbf{j} \right) \right] = -\frac{1}{\varepsilon_0} \left(\frac{\partial \rho}{\partial t} + \boldsymbol{\nabla} \cdot \mathbf{j} \right)$$

and we can observe that $\boldsymbol{\nabla} \cdot \mathbf{E} = \rho/\varepsilon_0$ is satisfied *if* the continuity equation is respected for all time steps. In its discrete form, the continuity equation is given by

$$\partial_t \rho |_{i,j,k}^{n+\frac{1}{2}} + \partial_x j_x |_{i,j,k}^{n+\frac{1}{2}} + \partial_y j_y |_{i,j,k}^{n+\frac{1}{2}} + \partial_z j_z |_{i,j,k}^{n+\frac{1}{2}} = 0 \,.$$

2.3.1 Current deposition

2.3.2 Stability

In order to study the stability of the Yee algorithm, we will take a closer look at the propagation of an electromagnetic wave in vacuum following Lehe (2018 15–26 January[b]).

In order to simplify the calculations, we will begin with the one dimensional case with the electric field on Ox and the magnetic field on Oy. In this case, the propagation of electromagnetic waves is described by equations (2.10), with the current density term dropped. With a more compact notation, this gives

$$\frac{B_{y_{k+1/2}}^{n+1/2} - B_{y_{k+1/2}}^{n-1/2}}{\Delta t} = -\frac{E_{x_{k+1}}^{n} - E_{x_k}^{n}}{\Delta z} \tag{2.13a}$$

$$\frac{E_{x_k}^{n+1} - E_{x_k}^{n}}{\Delta t} = -c^2 \frac{B_{y_{k+1/2}}^{n+1/2} - B_{y_{k-1/2}}^{n+1/2}}{\Delta z} \,. \tag{2.13b}$$

In order to better motivate the following derivation, let us consider the continuous (3D) case first. Equations (2.13) are the 1D discretisations of

$$\frac{\partial \mathbf{B}}{\partial t} = -\boldsymbol{\nabla} \times \mathbf{E}$$

$$\frac{1}{c^2} \frac{\partial \mathbf{E}}{\partial t} = \boldsymbol{\nabla} \times \mathbf{B} \,.$$

If we take the time derivative of the second equation, we obtain

$$\frac{1}{c^2}\frac{\partial^2 \mathbf{E}}{\partial t^2} = \frac{\partial}{\partial t}\boldsymbol{\nabla}\times\mathbf{B} = \boldsymbol{\nabla}\times\left(\frac{\partial\mathbf{B}}{\partial t}\right) = \boldsymbol{\nabla}\times(-\boldsymbol{\nabla}\times\mathbf{E}) = -\boldsymbol{\nabla}\underbrace{(\boldsymbol{\nabla}\cdot\mathbf{E})}_{0\text{ in vacuum}}+\nabla^2\mathbf{E}\,,$$

in which we can recognise the wave equation

$$\frac{1}{c^2}\frac{\partial^2\mathbf{E}}{\partial t^2}-\nabla^2\mathbf{E} = \square\,\mathbf{E} = 0\,.$$

Thus if we divide equation (2.13b) by c^2 and take the time derivative, we should obtain the discretised wave equation. Using centred time differences between equation (2.13b) at time step n and $n-1$, we obtain

$$\frac{1}{c^2}\frac{1}{\Delta t}\left(\frac{E_{xk}^{\,n+1}-E_{xk}^{\,n}}{\Delta t}-\frac{E_{xk}^{\,n}-E_{xk}^{\,n-1}}{\Delta t}\right) = \frac{1}{\Delta t}\left(-\frac{B_{yk+1/2}^{\,n+1/2}-B_{yk-1/2}^{\,n+1/2}}{\Delta z}+\frac{B_{yk+1/2}^{\,n-1/2}-B_{yk-1/2}^{\,n-1/2}}{\Delta z}\right).$$

The time and space derivatives commute, so we can rearrange the terms in the right hand side to match a centred time derivative and thus obtain

$$\frac{1}{c^2}\frac{E_{xk}^{\,n+1}-E_{xk}^{\,n}}{\Delta t^2}-\frac{1}{c^2}\frac{E_{xk}^{\,n}-E_{xk}^{\,n-1}}{\Delta t^2} = -\frac{B_{yk+1/2}^{\,n+1/2}-B_{yk-1/2}^{\,n+1/2}}{\Delta z\Delta t}+\frac{B_{yk+1/2}^{\,n-1/2}-B_{yk-1/2}^{\,n-1/2}}{\Delta z\Delta t}$$

$$= -\frac{B_{yk+1/2}^{\,n+1/2}-B_{yk+1/2}^{\,n-1/2}}{\Delta z\Delta t}+\frac{B_{yk-1/2}^{\,n+1/2}-B_{yk-1/2}^{\,n-1/2}}{\Delta z\Delta t}$$

$$= \frac{E_{xk+1}^{\,n}-E_{xk}^{\,n}}{\Delta z^2}-\frac{E_{xk}^{\,n}-E_{xk-1}^{\,n}}{\Delta z}\,,$$

where in the last step we used equation (2.13a). We can observe that the terms can be rearranged such that we obtain second order centred time derivatives. Thus we obtain the 1D discrete wave equation

$$\frac{1}{c^2}\frac{E_{xk}^{\,n+1}-2E_{xk}^{\,n}+E_{xk}^{\,n-1}}{\Delta t^2} = \frac{E_{xk+1}^{\,n}-2E_{xk}^{\,n}+E_{xk-1}^{\,n}}{\Delta z^2}\,. \tag{2.14}$$

We will now take a closer look at the behaviour of the propagating wave solutions

$$E_{xl}^{\,n} = E_0\,\mathrm{e}^{\mathrm{i}kl\Delta z-\mathrm{i}\omega n\Delta t}\,,$$

where we changed to using the l for indexing as not confuse it with the wavenumber k. Using this solution in equation (2.14) gives

$$\frac{E_0\,\mathrm{e}^{\mathrm{i}kl\Delta z}}{c^2}\frac{\mathrm{e}^{-\mathrm{i}\omega(n+1)\Delta t}-2\,\mathrm{e}^{-\mathrm{i}\omega n\Delta t}+\mathrm{e}^{-\mathrm{i}\omega(n-1)\Delta t}}{\Delta t^2} = E_0\,\mathrm{e}^{-\mathrm{i}\omega n\Delta t}\frac{\mathrm{e}^{\mathrm{i}k(l+1)\Delta z}-2\,\mathrm{e}^{\mathrm{i}kl\Delta z}+\mathrm{e}^{\mathrm{i}k(l-1)\Delta z}}{\Delta z^2}$$

$$\frac{\mathrm{e}^{\mathrm{i}kl\Delta z-\mathrm{i}\omega n\Delta t}}{c^2}\frac{\mathrm{e}^{-\mathrm{i}\omega\Delta t}-2+\mathrm{e}^{\mathrm{i}\omega\Delta t}}{\Delta t^2} = \mathrm{e}^{-\mathrm{i}\omega n\Delta t+\mathrm{i}kl\Delta z}\frac{\mathrm{e}^{\mathrm{i}k\Delta z}-2+\mathrm{e}^{-\mathrm{i}k\Delta z}}{\Delta z^2}$$

$$\frac{1}{c^2}\frac{\mathrm{e}^{-\mathrm{i}\omega\Delta t}-2+\mathrm{e}^{\mathrm{i}\omega\Delta t}}{\Delta t^2} = \frac{\mathrm{e}^{\mathrm{i}k\Delta z}-2+\mathrm{e}^{-\mathrm{i}k\Delta z}}{\Delta z^2}$$

$$\frac{1}{c^2\Delta t^2}\left(\mathrm{e}^{-\mathrm{i}\omega\Delta t/2}-\mathrm{e}^{\mathrm{i}\omega\Delta t/2}\right)^2 = \frac{1}{\Delta z^2}\left(\mathrm{e}^{-\mathrm{i}k\Delta z/2}-\mathrm{e}^{\mathrm{i}k\Delta z/2}\right)^2.$$

Using Euler's formula

$$\mathrm{e}^{\mathrm{i}x} = \cos x+\mathrm{i}\sin x\,,$$

35

we obtain

$$\frac{1}{c^2 \Delta t^2} \sin^2\left(\frac{\omega \Delta t}{2}\right) = \frac{1}{\Delta z^2} \sin^2\left(\frac{k \Delta z}{2}\right). \tag{2.15}$$

Equation (2.15) is a dispersion relation for the discrete one dimensional wave propagation. In the continuous case the dispersion relation is $\omega^2 = c^2 k^2$.

If we take the square root of equation (2.15)

$$\sin^2\left(\frac{\omega \Delta t}{2}\right) = \frac{c^2 \Delta t^2}{\Delta z^2} \sin^2\left(\frac{k \Delta z}{2}\right)$$

$$\left|\sin\left(\frac{\omega \Delta t}{2}\right)\right| = \left|\frac{c \Delta t}{\Delta z} \sin\left(\frac{k \Delta z}{2}\right)\right|$$

we observe that we obtain real solutions for ω, for any k

$$\omega = \pm \frac{2}{\Delta t} \arcsin\left(\frac{c \Delta t}{\Delta z} \sin\left(\frac{k \Delta z}{2}\right)\right)$$

only if $c \Delta t \leq \Delta z$.

Thus the phase velocity of electromagnetic waves $v_\phi = \omega/k$ will be given by

$$v_\phi = \pm \frac{2}{k \Delta t} \arcsin\left(\frac{c \Delta t}{\Delta z} \sin\left(\frac{k \Delta z}{2}\right)\right).$$

This means that in a 1D PIC code that is using the Yee discretisations, electromagnetic waves in vacuum propagate with a velocity depending on k, instead at the (constant) speed of light. This phenomena is called *numerical dispersion*. Since the wavenumber is inverse proportional to the wavelength, electromagnetic waves with shorter wavelengths will propagate slower.

For $c \Delta t \geq \Delta z$, the discrete dispersion relation given by equation (2.15) has no real solutions in the limit $k \to \pi/\Delta z$. The solution is imaginary and the corresponding mode is said to be unstable. As a consequence, PIC codes using FDTD methods like presented here are restricted to $c \Delta t \leq \Delta z$. This is called the *Courant limit*. This coupling between Δz and Δt places an upper bound on how fast can a simulation advance. Moreover, Δz is tightly coupled with the physics of the simulation, since it must be chose such that it can resolve the smallest features of the given problem.

This kind of analysis can be extended in a straightforward way to the 3D case. In this case the discrete version of the solution to the wave equation will be given by

$$E = E_0 \, \mathrm{e}^{ik_x x + ik_y y + ik_z z - i\omega t}.$$

Similarly, the 3D dispersion relation will be given by

$$\frac{1}{c^2 \Delta t^2} \sin^2\left(\frac{\omega \Delta t}{2}\right) = \frac{1}{\Delta x^2} \sin^2\left(\frac{k_x \Delta x}{2}\right) + \frac{1}{\Delta y^2} \sin^2\left(\frac{k_y \Delta y}{2}\right) + \frac{1}{\Delta z^2} \sin^2\left(\frac{k_z \Delta z}{2}\right)$$

and the 3D Courant condition by

$$c \Delta t \leq \frac{1}{\sqrt{\frac{1}{\Delta x^2} + \frac{1}{\Delta y^2} + \frac{1}{\Delta z^2}}}.$$

As we can see from the dispersion relation, in the 3D case, the phase velocity will depend on wavelength and propagation direction.

2.4   Particle in Cell codes in practice

In order to actually use the Particle in Cell method, a concrete implementation is needed. Since the beginning of the PIC method, several software packages were developed for simulations. Due to the complexity of the physical processes involved significant computational resources are required for PIC simulations and for this reason the performance of the program is very important.

2.4.1   A brief overview of HPC

With the advent of exa-scale computing, the performance of the systems and of the codes is mainly given by the scalability. Thus the ability to fully utilize the resources of a cluster or of a super-computer is critical to the usability of PIC codes. Particle in Cell codes thus fall in the category of High Performance Computing (HPC).

Theoretical description of scalability

The scalability of any code is achieved via efficient parallelisation and task scheduling on multiple levels. In order to measure how scalable a code is, we can compare its benchmarks with two theoretical scalability limits: Amdahl's law (Amdahl 1967) and Gustafson's law (Gustafson 1988).

Amdahl's law considers that a task can be split in a parallelisable part (p) and a serial part. If we consider the problem size fixed and we increase parallelisation, then the maximal speedup that can be achieved is limited by the part that cannot be parallelized $1 - p$.

If we consider the theoretical scaling of a program as a function of the number of processors n, then the speedup is given by

$$S_A = \frac{1}{(1 - p) + \frac{p}{n}} \qquad \text{and} \qquad \lim_{n \to \infty} S_A = \frac{1}{1 - p}.$$

Gustafson's law considers that with the increase of computational resources we can solve more complicated tasks in the same time. In this case, if s is the serial part of the task that does not benefit from parallelisation, then the speedup as a function of the number of processors n is

$$S_G = n + (1 - n)s = 1 - p + np.$$

As we can see in figure 2.4, Amdahl's law shows that adding more an more processors yields diminishing returns as we approach the limit. Note that in the above discussion we use the processor term in a generic fashion, not an actual processor which may have complicated architectural details. There are also several other assumptions such as the fact that the processors or parallel units are identical (of the same type) and that the cost of parallelisation is independent of the number of processors, but the most important assumption is the fact that the problem size is fixed. This is where Gustafson's law comes into place. As we can see in figure 2.5, its predictions about scaling are not so grim and it doesn't impose a limit on scaling. Instead of showing the limitations imposed by the serial parts of the programs, it shows that speedups can be achieved by increasing the problem size. Amdahl's law is also called strong scaling and Gustafson's law is also called weak scaling (Lin 2018). In figure 2.6 we can see a comparison between the two and the perfect scaling ($S_p(n) = n$). Scaling efficiency in the case of strong scaling is defined as

$$\eta_s = \frac{t_1}{n t_n},$$

where t_1 is the time for the task with one processor and t_n in the time for the task with n processors. In the case of weak scaling

$$\eta_w = \frac{t_1}{t'_n} \,,$$

where t_1 is the time required for the reference problem size, while t'_n is the time for a problem n times bigger computed with n processors (Shared Hierarchical Academic Research Computing Network 2016).

Practical aspects

Modern processors not only have multiple cores, but they also have special instruction sets that execute vectorized operations, these are generically called SIMD, which stands for Single Instruction, Multiple Data. Thus, in order to efficiently utilize the computational power of a single processor, instruction level parallelism must be combined with thread or process based parallelism, while parallelisation in itself is important, there are also several other critical factors that must be considered.

One important aspect is that of data availability. The processor must load data in order to make computations. It doesn't matter how fast is the processor is the data loading is inefficient. Data can be loaded from different sources. The fastest is the data already in the CPU caches, followed by the data loaded from RAM and other I/O (input/output) sources (hard drives or network for example). In order to have data available more efficiently modern processors use prefetching, that they load more data from the RAM in the processor cache in order to have faster access for subsequent queries. This aspects must be considered when writing simulation programs, since accessing data in a way that is not favorised by prefetching may lead to significant slowdowns from cache misses. The picture is more complicated with
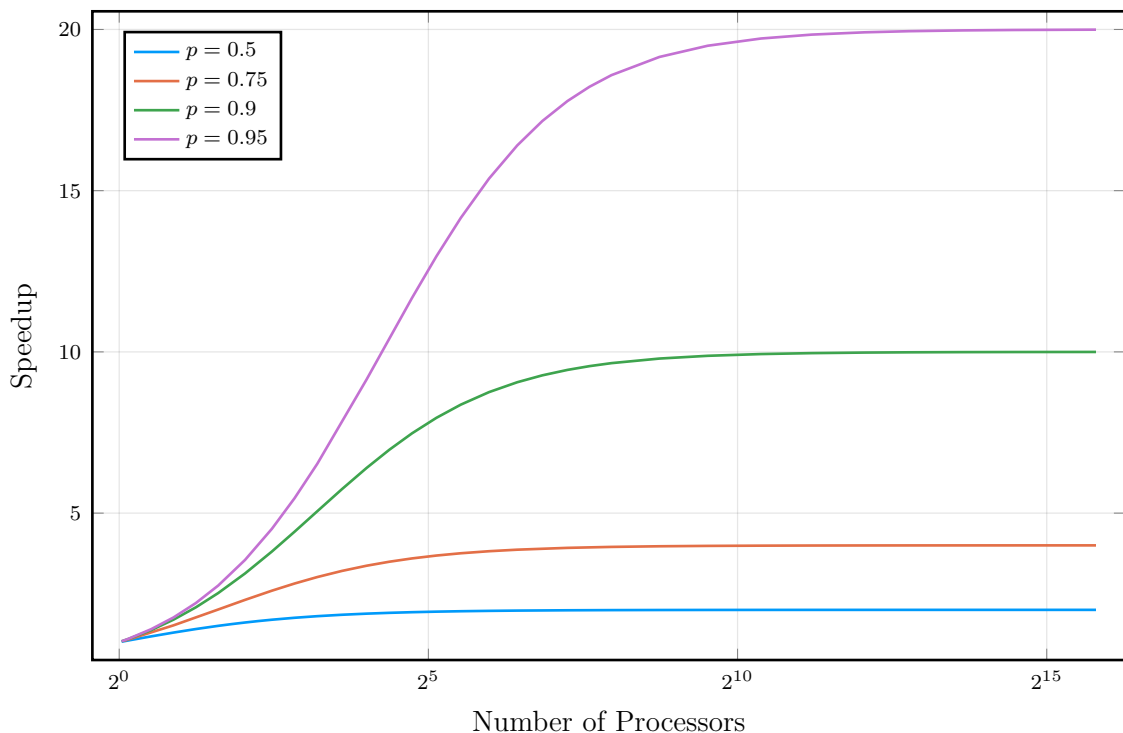

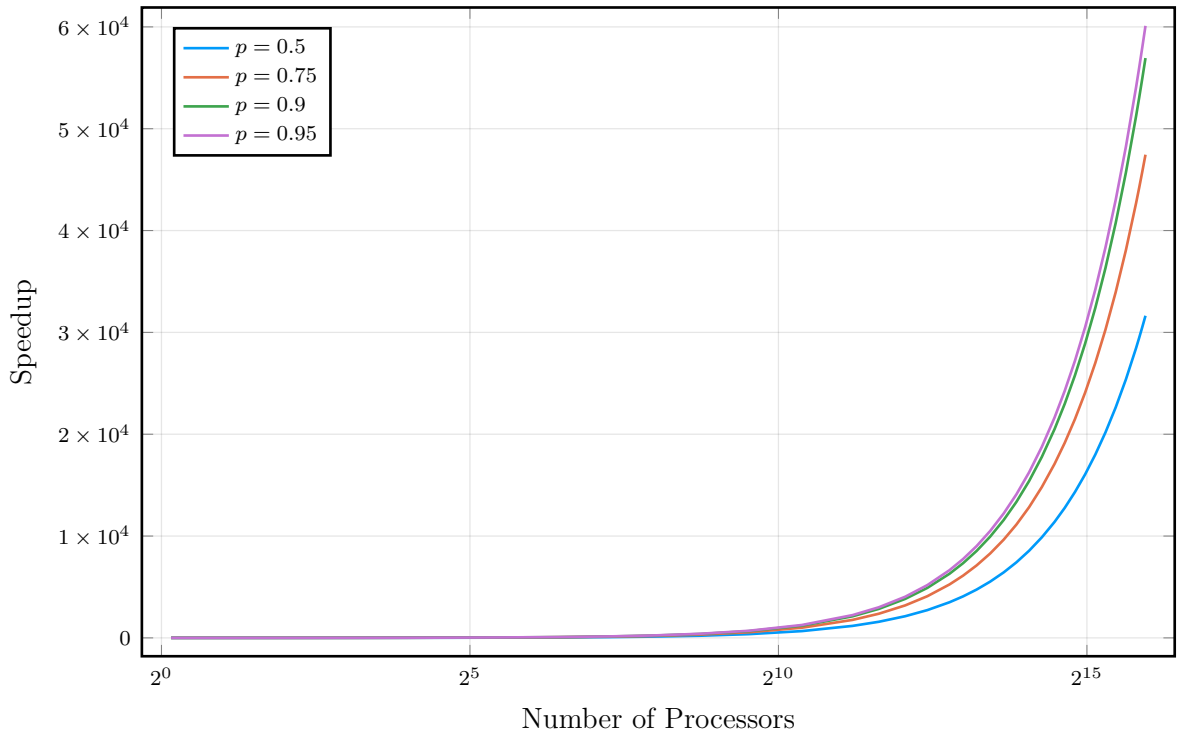Figure 2.4: The speedup computed with Amdahl's law

Figure 2.5: The speedup computed with Gustafson's law

parallelisation, as each processor has its own cache and care must be taken such that different cores must not race for the same memory region (this is called false sharing). Moreover, servers usually have multiple processors, each with several cores. These are just a few aspects that scratch the surface of the complexity involved in the parallelisation at the level of a single machine.

Moving on to multiple machines, network access between nodes becomes of critical importance for computing tasks that require frequent communication between nodes. In PIC code the simulation domain is split in several parts and each machine gets some parts of the domain that is responsible for. This process is called domain decomposition. In this case each machine can work independently to update the interior of its domain and must only communicate with its neighbours in order to update the boundaries. Thus, in PIC codes inter-process and inter-machine communication is very important. The important aspect for the network layer is low latency. This can be achieved by using technologies such as InfiniBand and RDMA. InfiniBand is a networking standard that provides very high throughput and very low latency and RDMA stands for Remote Direct Memory Access and as the name implies allows direct memory access form one machine into another without the involvement or overhead of the operations managed by the operating system. In order to address the challenge of creating programs that take advantage of such features, the MPI standard was developed. MPI stands for Message Passing Interface and it is a communication protocol for programming parallel computers.

While CPUs definitely play an important role in parallel computing, in the last decade GPUs and more recently other dedicated hardware accelerators, have become more and more important. Compared with CPUs, GPUs have a lot of cores, almost two to three order of magnitude more than common CPUs. While processors have few tens of cores, with state of the art reaching up to hundreds of cores (Intel Corporation 2016; IBM 2018; Vazhkudai *et al.* 2018), GPUs can reach over 5000 cores (NVIDIA Corporation 2018a). One important aspect is that GPUs cores have simpler architecture compared with processors, usually favour
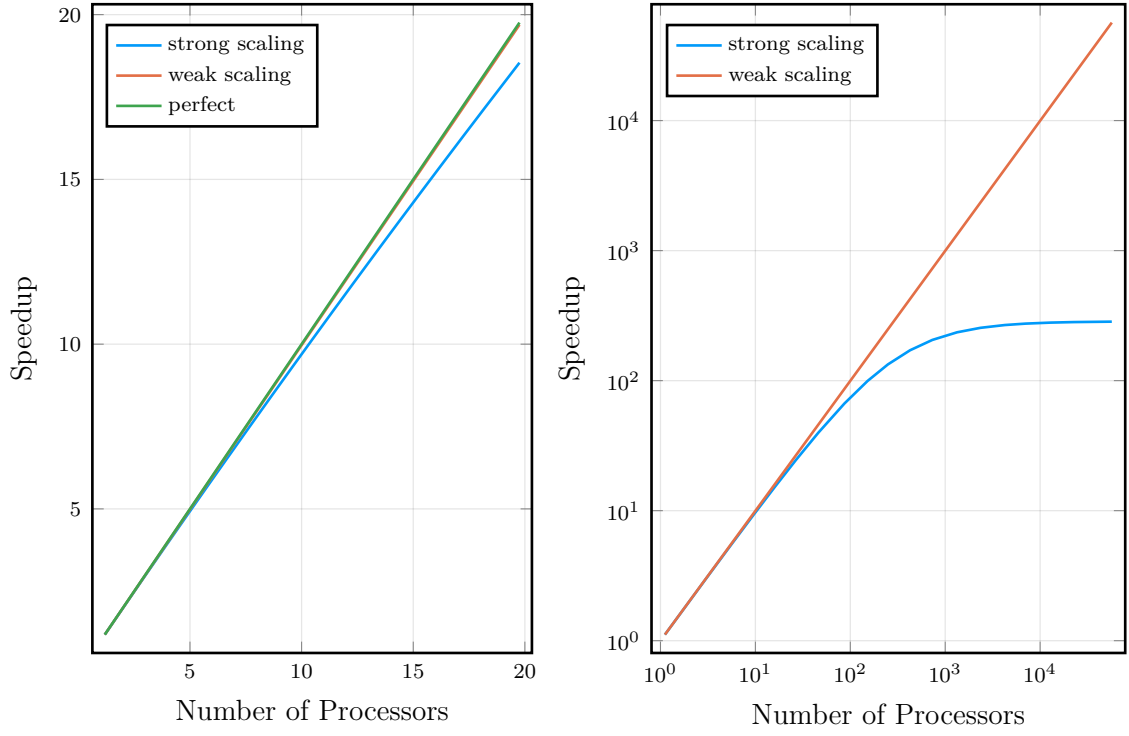
Figure 2.6: The theoretical speedup compared with linear axis and small number of processors on the left and log-log scale with a large number of processors on the right

single precision computations, and have much less memory. While CPUs processors can have access to hundreds of Gigabytes of RAM memory, GPUs usually have a few tens Gigabytes of memory, state of the art units reaching near one hundred (Vazhkudai *et al.* 2018). Thus, loading data efficiently into the GPU memory represents a critical aspect that must be considered. In combination with the networking layer, this yields new performance problems that need to be addressed. In order to address these challenges, technologies such as NVIDIA® NVLink™ have been developed, that allow direct GPU to GPU communication (NVIDIA Corporation 2018b).

2.4.2 A survey of available PIC codes

As a concrete example of scalability in PIC codes, we will consider Osiris (Fonseca, Silva, *et al.* 2002), a three dimensional, fully relativistic Particle in Cell code. Fonseca, Vieira, *et al.* (2013) benchmarked Osiris on Top 500 (Strohmaier, Dongarra, and Simon 1993–2019) supercomputers including the Jaguar system at Oak Ridge National Laboratory and the Sequoia system at Lawrence Livermore Laboratory in the US. The main result is the very good scaling behaviour of the Osiris code from 4096 cores to 1572864 cores on the Sequoia system, as can be seen in figure 2.7. Note that in order to compare the results with the theoretical descriptions for strong and weak scaling, one has to adjust the formulae in order to account for the fact that the processor number does not start with 1, *i.e.* $S(4096) = 1$. In order to achieve this performance, the code had to be heavily optimised over multiple levels of parallelism. Besides MPI they used shared memory parallelism and instruction level parallelism in order to fully benefit from the available computing power. Besides advanced implementation techniques such as the SIMD vectorised particle pusher, an important role is given by the nature of the algorithms and thus using methods that only require local state information is crucial for scalability. As an example, the FDTD method for updating the fields, only requires information from its neighbours as

opposed to classical spectral methods that require the global state information.

Another important aspect stressed in the previously mentioned article, is that of load balancing. For highly non-linear applications such as Laser Wakefield acceleration, regions of very high particle density are of critical importance for the physical phenomena, but they create a very high load imbalance in the simulation. One solution that was investigated was the use of shared memory parallelism which offset the imbalance by using more threads on the machines that have to deal with high density regions. Another approach was of algorithmic nature, by using dynamical load balancing in order to adjust the domain boundaries.

While performance and scaling are important properties of a PIC code, the ability to realistically simulate the physics of the phenomena is of paramount importance. Using charge conserving schemes for current deposition and higher order splines for shape functions contributes to better accuracy, and support for ionization, collisions and QED effects gives a better representations of the physics simulations. Both of these aspects are required for solving complex problems such as accelerator design.

Another state of the art PIC code is Warp-X (J.-L. Vay *et al.* 2018), which is a framework for laser plasma simulations in the context of accelerator design. It combines three software components: Warp (a framework for modelling plasma and particle accelerators), AMRex (Adaptive Mesh Refinement library) and PICSAR (low level PIC primitives). It is designed for running at exa-scale and has advanced features such as ultrahigh-order pseudo-spectral analytical time-domain (PSATD) field solvers (Vincenti and Jean-Luc Vay 2018) and multiple ionisation modes.

The Extreme Light Infrastructure

The Extreme Light Infrastructure (ELI) project is a pan-European research infrastructure dedicated to ultra-intense and ultra-short laser pulses (Gales 2016). The ELI facility consists of three pillars built in The Czech Republic, Hungary and Romania, with the Romanian pillar being ELI-Nuclear Physics (ELI-NP). One of the proposed experiments is the experimental demonstration of the QED-plasma regime, which involves radiation damping due to the synchrotron radiation (Turcu *et al.* 2016). One of the key signatures for this effect is given by the scaling of energetic photon emission with peak laser intensity. Particle in Cell simulations using the EPOCH program (Arber *et al.* 2015) were used to predict an increase in γ-ray emission at high laser intensities such as 10^{21}–$10^{22}\,\mathrm{W\,cm^{-2}}$, due to the additional synchrotron component (Brady *et al.* 2014).

Another ELI project concerns the development of the ion sources such that GeV protons could be obtained at the limit of the ELI parameters, *i.e.* using laser intensities in the range of $10^{24}\,\mathrm{W\,cm^{-2}}$. Particle in Cell simulations with the Osiris program were used to find the laser parameters corresponding to the ion source at the $100\,\mathrm{PW}$ range (Mourou *et al.* 2011, p. 327).

Frequently used codes

A list of frequently used simulation programs is given in table 2.1. This list is by no means exhaustive, but it should provide an overview of how different features are adopted in PIC codes. The codes are organized considering their features and implementation features. For the features, the "Type" column indicates whether the code is electromagnetic (solves Maxwell's equations) or quasi-static (solves Poisson's equation), and available simulation features such as different geometries or special field solvers. The "Scalability" column is dedicated to implementation details that are strongly related to how scalable the code is. Thus, for inter-node and inter-process communication MPI is generally used, for shared memory parallelism OpenMP or
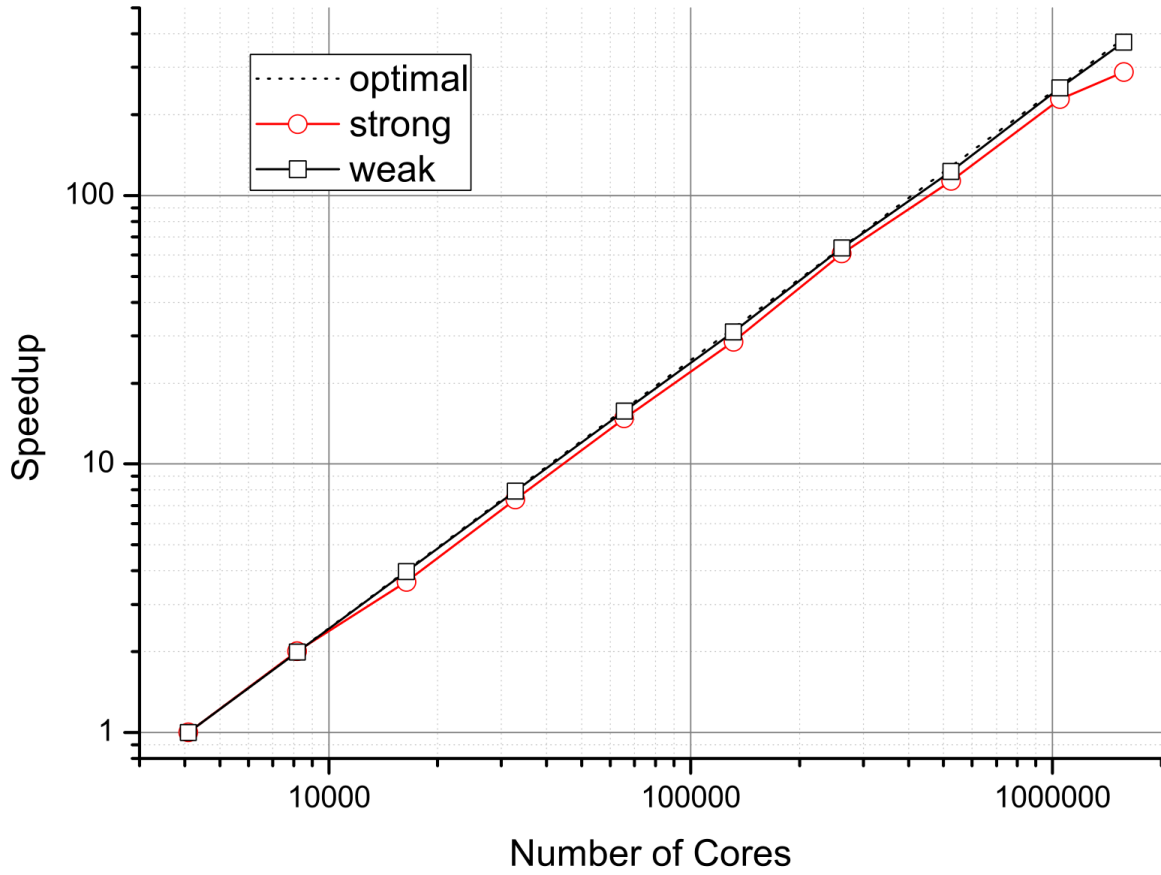
Figure 2.7: The scaling behaviour of Osiris at the Sequoia system at Lawrence Livermore Laboratory. Figure 5 reproduced from Fonseca, Vieira, *et al.* (2013).

pthreads are widely used. For GPU specific tasks, the CUDA framework is used in conjunction with NVIDIA hardware. While a significant portion of the codes is written in `Fortran`, `C` or `C++`, there are some codes written in `Python`, or with `Python` wrappers. In this case NUMBA, an open source JIT (Just In Time) compiler, is usually used to enhance performance by translating a subset of `Python` and `NumPy` into LLVM code. `NumPy` is an optimized array library in `Python` for working with N-dimensional arrays and LLVM stands for Low Level Virtual Machine and it is a compiler infrastructure that can be used to emit optimized machine code. A recent trend in HPC is the rise of heterogeneous computing, involving mainly CPUs and GPUs, and thus the "GPU ready" column was included to indicate the adoption of this computing model among various programs.

In table 2.1 we used the following abbreviations

- EM: Electromagnetic PIC

- QS: Quasi-Static PIC

- 3D: Cartesian coordinates, up to 3D

- RZ: Cylindrical geometry with FDTD method in r and z directions

- RZ$^{\text{F}}$: Cylindrical geometry with Fourier azimuthal decomposition

- RZ$^{\text{FFT}}$: Cylindrical geometry with FDTD method in r direction and FFT-based pseudo-spectral method in z direction

Name	Type	GPU ready	Scalability
EPOCH	EM 3D	No	MPI
Osiris	EM 3D, RZ$^\text{F}$, RZ$^\text{FFT}$	Yes	MPI, OpenMP, SIMD
Warp-X	EM 3D, PS, RZ$^\text{F}$, RZ$^\text{FFT}$	Yes	MPI, OpenMP, SIMD
PIConGPU	EM 3D	Yes	MPI, CUDA-ALPAKA
VSim	EM 3D	Yes	MPI
FBPIC	EM 3D, RZ$^\text{H}$	Yes	MPI, NUMBA
VPIC	EM 3D	No	MPI, pthreads, SIMD
QuickPIC	QS RZ	No	MPI
PICLS	EM 3D	No	MPI

Table 2.1: Commonly used simulation programs

- RZ$^\text{H}$: Cylindrical geometry with Henkel transform in r direction and FFT-based pseudo-spectral method in z direction

- PS: Pseudo-spectral Maxwell solver with domain decomposition and local Fourier transform

2.5 EPOCH

EPOCH (Arber *et al.* 2015) is a plasma simulation code using the Particle in Cell method featuring dynamic load balancing, parallel I/O based on MPI, and integration with a wide array of visualisation tools. The EPOCH user manual (Bennett *et al.* 2019) provides the required information for installing and utilizing the code.

EPOCH uses input files, also called input decks in order to configure the simulation parameters and the choice of solvers. The input deck contains several blocks, each considering a specific aspect. We will quickly present some of the main blocks

- The "control" block: this block contains general information concerning the geometry of the simulation domain, the load balancing method, the initial conditions and the algorithm choice for the field solver.

- The "boundaries" block: this block provides the details regarding boundary condition handling.

- The "species" block: this block is used to specify the particle species to be used in the simulation and their properties.

- The "laser" block: this block provides the information about the laser source.

- The "fields" block: this block contains the specifics of the electromagnetic fields present at the start of the simulation.

- The "window" block: this block can be used in order to create a moving window in which the simulation occurs. This can be useful in cases where the simulation domain is large, but the interesting part is relatively small (and can be followed during the evolution).

- The "output" block: this block is used to specify where and how often to write the output files.

The output of EPOCH simulations is given in a custom file format, SDF (Self Describing Format). EPOCH provides several reader plugins for `ITT`, `IDL`, `LLNL VisIt`, `Mathworks Matlab` and `Python`. The output files written to disk, also called output dumps, can be of several types, with varying degrees of detail. The most detailed one, called the restart dump can be used to restart the simulation at a later time. The quantities to be written can have some filters, called dumpmasks, indicating the output frequency and level of detail. The output information provided by EPOCH can be grouped in four categories: particle variables, grid variables, derived variables and other variables.

Particle variables include

- the position of the particles

- the momenta and velocities of the particles

- the charge and mass of the particles

- the particle weight, representing how much real particles does a pseudo-particle represent

- the particle energy

- the work excreted by the fields on the particle

Grid variables include

- the locations of the grid points

- the electric and magnetic field values

- the current density values

Derived variables include

- the average particle energy

- the mean energy flux on the grid

- the mass and charge density

- the number density

- the number of particles per cell

- the average particle weight per cell

- the average momenta of the particles per cell

- the temperature on the grid

- the Poynting vector flux

Chapter 3

Results

Add something

Chapter 4

Conclusions

In this thesis we have studied ...

Bibliography

Tajima, T. and J. M. Dawson (July 23, 1979). "Laser Electron Accelerator". In: *Physical Review Letters* 43.4, pp. 267–270. DOI: 10.1103/PhysRevLett.43.267.

Jackson, John David (1999). *Classical Electrodynamics*. 3rd ed. New York: Wiley. 808 pp. ISBN: 978-0-471-30932-1.

Eisenberg, Judah M. and Walter Greiner (1978). *Nuclear Theory. 2: Excitation Mechanisms of the Nucleus*. 2., rev. ed., 1. repr. OCLC: 256795525. Amsterdam: North-Holland [u.a.] 421 pp. ISBN: 978-0-7204-0483-8.

Karsch, Stefan (2018). "Applications of High Intensity Laser Pulse". Lecture Notes. Lecture Notes. Ludwig-Maximilians-University Munich. URL: https://www.physik.uni-muenchen.de/lehre/vorlesungen/sose_18/applications_of_high-intensity_laser-pulses/vorlesung/LaserMatter.pdf (visited on 06/09/2019).

Arber, T D *et al.* (Nov. 1, 2015). "Contemporary Particle-in-Cell Approach to Laser-Plasma Modelling". In: *Plasma Physics and Controlled Fusion* 57.11, pp. 1–26. ISSN: 0741-3335, 1361-6587. DOI: 10.1088/0741-3335/57/11/113001.

Hockney, Roger W. and James W. Eastwood (1988). *Computer Simulation Using Particles*. Special student ed. Bristol [England]; Philadelphia: A. Hilger. 540 pp. ISBN: 978-0-85274-392-8.

Butcher, J. C. (2016). *Numerical Methods for Ordinary Differential Equations*. Third edition. Chichester, West Sussex, United Kingdom: Wiley. 513 pp. ISBN: 978-1-119-12150-3.

Leimkuhler, B. and Sebastian Reich (2004). *Simulating Hamiltonian Dynamics*. Cambridge Monographs on Applied and Computational Mathematics 14. Cambridge, UK; New York: Cambridge University Press. 379 pp. ISBN: 978-0-521-77290-7.

Buneman, O (June 1967). "Time-Reversible Difference Procedures". In: *Journal of Computational Physics* 1.4, pp. 517–535. ISSN: 00219991. DOI: 10.1016/0021-9991(67)90056-3.

Birdsall, Charles K and A. Bruce Langdon (2005). *Plasma Physics via Computer Simulation*. Series in Plasma Physics. OCLC: 968173834. Bristol: Institute of Physics Pub. ISBN: 978-1-4822-6306-0. URL: http://public.eblib.com/choice/publicfullrecord.aspx?p=1675636 (visited on 06/21/2019).

Boris, Jay P. (Nov. 2, 1970). "Relativistic Plasma Simulation–Optimization of a Hybrid Code". In: *Fourth Conference on Numerical Simulations of Plasmas*. Naval Research Laboratory, Washington, D.C.: Defense Technical Information Center, pp. 3–67. URL: http://archive.org/details/DTIC_ADA023511 (visited on 08/07/2019).

Stuart, A. M. and A. R. Humphries (1996). *Dynamical Systems and Numerical Analysis*. Cambridge Monographs on Applied and Computational Mathematics 2. Cambridge; New York: Cambridge University Press. 685 pp. ISBN: 978-0-521-49672-8.

Qin, Hong *et al.* (Aug. 1, 2013). "Why Is Boris Algorithm so Good?" In: *Physics of Plasmas* 20.8, p. 084503. ISSN: 1070-664X. DOI: 10.1063/1.4818428.

Arnol'd, V. I. (1989). *Mathematical Methods of Classical Mechanics*. 2nd ed. Graduate Texts in Mathematics. New York: Springer-Verlag. ISBN: 978-0-387-96890-2. URL: `https://www.springer.com/gp/book/9780387968902` (visited on 08/11/2019).

Golomb, Solomon W. (Mar. 1, 1985). "Proof without Words: A 2×2 Determinant Is the Area of a Parallelogram". In: *Mathematics Magazine* 58.2, p. 107. ISSN: 0025570X. DOI: `10.2307/2689900`. JSTOR: `10.2307/2689900?origin=crossref`.

Hairer, Ernst, Christian Lubich, and Gerhard Wanner (2006). *Geometric Numerical Integration: Structure-Preserving Algorithms for Ordinary Differential Equations*. 2nd ed. Springer Series in Computational Mathematics 31. OCLC: ocm69223213. Berlin; New York: Springer. 644 pp. ISBN: 978-3-540-30663-4.

Marsden, Jerrold E. and Tudor S. Ratiu (1999). *Introduction to Mechanics and Symmetry: A Basic Exposition of Classical Mechanical Systems*. Red. by Jerrold E. Marsden *et al.* Vol. 17. Texts in Applied Mathematics. New York, NY: Springer New York. ISBN: 978-1-4419-3143-6 978-0-387-21792-5. DOI: `10.1007/978-0-387-21792-5`. URL: `http://link.springer.com/10.1007/978-0-387-21792-5` (visited on 08/10/2019).

Hairer, Ernst and Christian Lubich (Dec. 2018). "Energy Behaviour of the Boris Method for Charged-Particle Dynamics". In: *BIT Numerical Mathematics* 58.4, pp. 969–979. ISSN: 0006-3835, 1572-9125. DOI: `10.1007/s10543-018-0713-1`.

Higuera, A. V. and J. R. Cary (Apr. 24, 2017). "Structure-Preserving Second-Order Integration of Relativistic Charged Particle Trajectories in Electromagnetic Fields". In: *Physics of Plasmas* 24.5, p. 052104. ISSN: 1070-664X. DOI: `10.1063/1.4979989`.

Kane Yee (May 1966). "Numerical Solution of Initial Boundary Value Problems Involving Maxwell's Equations in Isotropic Media". In: *IEEE Transactions on Antennas and Propagation* 14.3, pp. 302–307. ISSN: 0018-926X. DOI: `10.1109/TAP.1966.1138693`.

Lehe, Remi (2018 15–26 January[a]). "Electromagnetic Particle-In-Cell Codes". Lecture notes. USPAS 2018: Simulation of Beam and Plasma Systems (Old Dominion University Hampton, VA). URL: `https://people.nscl.msu.edu/~lund/uspas/sbp_2018/lec_em_pic/A1a_EM_PIC.pdf` (visited on 08/15/2019).

— (2018 15–26 January[b]). "Electromagnetic Wave Propagation in Particle-In-Cell Codes". Lecture notes. USPAS 2018: Simulation of Beam and Plasma Systems (Old Dominion University Hampton, VA). URL: `https://people.nscl.msu.edu/~lund/uspas/sbp_2018/lec_em_pic/A1b_EM_Waves.pdf` (visited on 08/15/2019).

Amdahl, Gene M. (1967). "Validity of the Single Processor Approach to Achieving Large Scale Computing Capabilities". In: *Proceedings of the April 18-20, 1967, Spring Joint Computer Conference* (Atlantic City, New Jersey). AFIPS '67 (Spring). New York, NY, USA: ACM Press, pp. 483–485. DOI: `10.1145/1465482.1465560`.

Gustafson, John L. (May 1988). "Reevaluating Amdahl's Law". In: *Commun. ACM* 31.5. Citation Key Alias: gustafson_reevaluatingamdahl_1988a, pp. 532–533. ISSN: 0001-0782. DOI: `10.1145/42411.42415`.

Lin, Xin (Nov. 9, 2018). *Scalability: Strong and Weak Scaling*. URL: `https://www.kth.se/blogs/pdc/2018/11/scalability-strong-and-weak-scaling/` (visited on 08/29/2019).

Shared Hierarchical Academic Research Computing Network (Mar. 1, 2016). *Measuring Parallel Scaling Performance - Documentation*. URL: `https://www.sharcnet.ca/help/index.php/Measuring_Parallel_Scaling_Performance#Calculating_Strong_Scaling_Efficiency` (visited on 08/30/2019).

Intel Corporation (2016). *Intel® Xeon Phi™ Processor 7290F (16GB, 1.50 GHz, 72 Core) Product Specifications*. URL: `https://ark.intel.com/content/www/us/en/ark/products/95831/intel-xeon-phi-processor-7290f-16gb-1-50-ghz-72-core.html` (visited on 08/26/2019).

IBM (2018). *POWER9 Servers Overview*. URL: https://www.ibm.com/downloads/cas/KDQRVQRR (visited on 08/26/2019).

Vazhkudai, S. S. *et al.* (July 30, 2018). *The Design, Deployment, and Evaluation of the CORAL Pre-Exascale Systems*. LLNL-CONF-755733. Lawrence Livermore National Lab. (LLNL), Livermore, CA (United States). URL: https://www.osti.gov/biblio/1489443-design-deployment-evaluation-coral-pre-exascale-systems (visited on 08/26/2019).

NVIDIA Corporation (2018a). *NVIDIA TESLA V100 GPU ACCELERATOR*. URL: https://images.nvidia.com/content/technologies/volta/pdf/tesla-volta-v100-datasheet-letter-fnl-web.pdf (visited on 08/26/2019).

— (2018b). *NVIDIA NVLink Fabric: Advanced Multi-GPU Processing*. URL: https://www.nvidia.com/en-us/data-center/nvlink/ (visited on 08/26/2019).

Fonseca, R. A., L. O. Silva, *et al.* (2002). "OSIRIS: A Three-Dimensional, Fully Relativistic Particle in Cell Code for Modeling Plasma Based Accelerators". In: *Computational Science — ICCS 2002*. Ed. by Peter M. A. Sloot *et al.* Lecture Notes in Computer Science. Springer Berlin Heidelberg, pp. 342–351. ISBN: 978-3-540-47789-1.

Fonseca, R. A., J. Vieira, *et al.* (Nov. 2013). "Exploiting Multi-Scale Parallelism for Large Scale Numerical Modelling of Laser Wakefield Accelerators". In: *Plasma Physics and Controlled Fusion* 55.12, p. 124011. ISSN: 0741-3335. DOI: 10.1088/0741-3335/55/12/124011.

Strohmaier, Erich, Jack Dongarra, and Horst Simon (1993–2019). *TOP500 Supercomputer Sites*. URL: https://www.top500.org/ (visited on 08/28/2019).

Vay, J.-L. *et al.* (Nov. 12, 2018). "Warp-X: A New Exascale Computing Platform for Beam–Plasma Simulations". In: *Nuclear Instruments and Methods in Physics Research Section A: Accelerators, Spectrometers, Detectors and Associated Equipment*. 3rd European Advanced Accelerator Concepts Workshop (EAAC2017) 909, pp. 476–479. ISSN: 0168-9002. DOI: 10.1016/j.nima.2018.01.035.

Vincenti, Henri and Jean-Luc Vay (July 1, 2018). "Ultrahigh-Order Maxwell Solver with Extreme Scalability for Electromagnetic PIC Simulations of Plasmas". In: *Computer Physics Communications* 228, pp. 22–29. ISSN: 0010-4655. DOI: 10.1016/j.cpc.2018.03.018.

Gales, S (2016). "Introduction". In: *Romanian Reports in Physics* 68 (Supplement), S5–S10. URL: http://www.rrp.infim.ro/2016_68_S/S5.pdf (visited on 08/29/2019).

Turcu, I C E *et al.* (2016). "High Field Physics and Qed Experiments at ELI-NP". In: *Romanian Reports in Physics* 68 (Supplement), S145–S231. URL: http://www.rrp.infim.ro/2016_68_S/S145.pdf (visited on 08/29/2019).

Brady, C. S. *et al.* (Mar. 1, 2014). "Synchrotron Radiation, Pair Production, and Longitudinal Electron Motion during 10-100 PW Laser Solid Interactions". In: *Physics of Plasmas* 21.3, p. 033108. ISSN: 1070-664X. DOI: 10.1063/1.4869245.

Mourou, Gérard A. *et al.*, eds. (2011). *ELI - Extreme Light Infrastructure WHITEBOOK*. Wolfshagener Str. 56 13187, Berlin, Germany: THOSS Media GmbH. 536 pp.

Bennett, Keith *et al.* (June 18, 2019). *Users Manual for the EPOCH PIC Codes*. University of Warwick. 147 pp. URL: https://cfsa-pmw.warwick.ac.uk/EPOCH/epoch/wikis/uploads/c2f6011459fb52017d6c78b0e87b4de9/epoch_user-4.17.pdf (visited on 08/31/2019).